

12-5-2018 10:00 AM

Investigating the role of endogenous ATF4 upregulation on neuronal glutathione level

Fatemeh Mirshafiei, *The University of Western Ontario*

Supervisor: Cregan, Sean, *The University of Western Ontario*

A thesis submitted in partial fulfillment of the requirements for the Master of Science degree in Neuroscience

© Fatemeh Mirshafiei 2018

Follow this and additional works at: <https://ir.lib.uwo.ca/etd>



Part of the [Medical Cell Biology Commons](#), and the [Neurosciences Commons](#)

Recommended Citation

Mirshafiei, Fatemeh, "Investigating the role of endogenous ATF4 upregulation on neuronal glutathione level" (2018). *Electronic Thesis and Dissertation Repository*. 5974.
<https://ir.lib.uwo.ca/etd/5974>

This Dissertation/Thesis is brought to you for free and open access by Scholarship@Western. It has been accepted for inclusion in Electronic Thesis and Dissertation Repository by an authorized administrator of Scholarship@Western. For more information, please contact wlsadmin@uwo.ca.

Abstract

ATF4 is a transcription factor that is activated in response to integrated stress response (ISR). In neurons specifically, ATF4 has been suggested to act as a pro-apoptotic transcription factor. The expression of ATF4, as well as its downstream gene targets have been implicated in both *in vivo* and *in vitro* models of Alzheimer's and Parkinson's Disease. However, the mechanism by which ATF4 promotes cell death remains unclear. It was previously shown that overexpression of ATF4 in primary cortical neurons caused a reduction in glutathione levels, resulting in oxidative stress-induced cell death. The aim of this project was to investigate whether endogenous upregulation of ATF4 during ER-stress-induced activation of the ISR affects GSH levels and neuronal survival, and to identify factors that might mediate this response. Our results showed that in the presence of ER stress, WT cells possibly degrade GSH more rapidly compared to ATF4-deficient neurons, however, they compensate for this by increasing the rate of GSH *de novo* synthesis and maintain higher levels of GSH. Our findings also showed that the ATF4-dependent cell death observed in TG treated neurons is not induced by oxidative stress and cannot be ameliorated by the addition of antioxidants. Finally, we suggest that the underlying reason behind our differential observation regarding GSH consumption in overexpression and endogenous ISR activation pathways, is due to context dependent induction of different ATF4 target genes.

Keywords

Activating transcription factor 4, ATF4, Oxidative stress, ER-stress, Glutathione, Neuron

Acknowledgments

I would first like to thank Dr. Sean Cregan, for taking me in as an international student and for supporting me in my growth as a scientist. As a supervisor, Dr. Cregan was always available and I could not have done this without his support, patience and guidance. I would also like to thank the members of my advisory committee, Dr. Peter Chidiac and Dr. Robert Cumming, for sharing their expertise with me and for providing me with ideas to help make my research better.

During the course of this masters, I have had the pleasure of meeting and befriending some exceptional individuals who have truly made this master's a memorable and special experience. I would especially like to thank all members of the Cregan lab: our lab technician, Heather Tarnowski- Garner, other fellow graduate students, undergraduate thesis students and undergraduate work/study students for making this experience truly exceptional. I would like to express my deepest appreciation to my dear friend and colleague, Vidhyasree Shyam, for her endless emotional support and for being there for me since day one. I consider myself fortunate to have met an amazing soul, and I could not think of a person more fit than her to have shared this experience with.

I would also like to extend my gratitude to Dr. Asit Rai for providing me with the technical expertise whenever I needed them and to Asad Lone for patiently helping me with my Seahorse experiments.

Last, but not least, I would like to thank my friends and family who supported me and motivated me through this process.

All the above-mentioned people were important pieces of my journey and my experience would not have been the same without them.

Table of Contents

Abstract	i
Acknowledgments.....	ii
Table of Contents	iii
List of Figures	vi
List of Appendices	viii
List of abbreviations	ix
Chapter 1	1
1 Introduction	1
1.1 Oxidative stress: The balance between free radicals and antioxidants	1
1.1.1 Free Radical	1
1.1.2 Antioxidants.....	2
1.2 Oxidative stress and neurodegeneration	10
1.2.1 Aging and oxidative damage	10
1.2.2 Alzheimer's disease	11
1.2.3 Parkinson's disease	12
1.2.4 Stroke	13
1.3 The role of integrated stress response during cellular stress.....	14
1.3.1 Activating Transcription Factor 4.....	17
1.3.2 The role of ISR and ATF4 expression in neurons	21
1.4 Rationale	23
1.5 Hypothesis.....	24
Chapter 2.....	26
2 Materials and Methods.....	26
2.1 Animals	26

2.1.1	Genotyping.....	26
2.2	Cell culture.....	26
2.2.1	Primary cortical neurons	26
2.2.2	N2A Cell line	27
2.2.3	Plasmid transfection.....	28
2.2.4	Drugs.....	28
2.3	Protein extraction and quantification	28
2.4	Glutathione assay	29
2.5	NADPH quantification.....	29
2.6	Mitochondrial ROS detection	30
2.7	Real time quantitative RT-PCR analysis	31
2.8	Metabolic flux assay	31
2.9	Cell death and survival assays	32
2.10	Fluorescent immunocytochemistry	32
2.11	Western blot analysis	33
2.12	Data analysis	33
Chapter 3	34
3	Results	34
3.1	Primary cortical cultures from both wildtype and ATF4-deficient mice are mainly neuronal.....	34
3.2	Wildtype neurons retain GSH more efficiently compared to ATF4-KO cells in the presence of ER-stress.....	36
3.3	ATF4 ^{+/+} neurons consume GSH more rapidly compared to ATF4-deficient cells in the presence of ER-stress	36
3.4	GSH regeneration pathway is not affected by ATF4 in neurons	40
3.5	ATF4 does not affect mitochondrial ROS production.....	42
3.5.1	ER-stress affects mitochondrial bioenergetics in an ATF4-independent manner.....	42

3.5.2	ER-stress induces mitochondrial superoxide production is independent of ATF4 upregulation.....	42
3.6	Endogenous ATF4 upregulation affects the gene expression profile of GSH related factors.....	46
3.7	Replenishment of the antioxidant pool does not protect neurons against ER-stress-induced cell death	47
3.8	ATF4 protein levels can be upregulated/stabilized in the presence or absence of ISR	52
3.9	Downstream target genes that are induced by ATF4 differ, depending on how ATF4 is expressed or stabilized.....	52
Chapter 4	57
4	Discussion	57
4.1	ATF4 plays a role in GSH synthesis.....	57
4.2	ATF4-dependent cell death under ER-stress conditions is independent of antioxidant depletion.....	60
4.3	ATF4 induces different target genes depending on how it's stabilized/ expressed	61
Chapter 5	63
5	Conclusion	63
References	64
Appendices	81
Curriculum Vitae	83

List of Figures

Figure 1.1. Free radical production in neurons	4
Figure 1.2. Glutathione system	9
Figure 1.3. Integrated stress response (ISR) regulates translation initiation and allows for translation of ATF4.....	16
Figure 1.4. Functional domains of ATF4 protein	19
Figure 1.5. Rationale and hypothesis.....	25
Figure 3.1. Primary cortical cultures are mainly neuronal.....	35
Figure 3.2. ATF4 ^{+/+} neurons retain GSH levels to a greater extent compared to ATF4 ^{-/-} neurons after induction of prolonged ER-stress.....	38
Figure 3.3. Endogenous upregulation of ATF4 increases GSH consumption.....	39
Figure 3.4. GSH regeneration pathway is not affected by ATF4	41
Figure 3.5. TG treatment affects mitochondrial bioenergetics in an ATF4-independent manner.....	43
Figure 3.6. Mitochondrial superoxide production is independent of ATF4 upregulation	45
Figure 3.7. ATF4 upregulation causes differential transcription of GSH-related genes	49
Figure 3.8. Replenishment of the antioxidant pool does not protect neurons against cell death	51
Figure 3.9. ATF4 protein levels are increased in response to various treatments	54
Figure 3.10. Downstream target genes that are induced by ATF4 differ, depending on the cell type and mechanism of ATF4 expression.....	55

Figure 3.11. The mechanism of ATF4 expression affects the induction of GSH related
transcripts. 56

List of Appendices

Appendix A. NADPH reaction mix	81
Appendix B. qRT-PCR primer list.....	82

List of abbreviations

6-OHDA	6-Hydroxydopamine
4E-BP1	Eukaryotic translation initiation factor 4E-binding protein 1
A β	Amyloid beta
AD	Alzheimer's disease
APP/PS-1	Amyloid precursor protein/preseilin-1
ASNS	Asparagine Synthetase
ATF3	Activating transcription factor 3
ATF4	Activating transcription factor 4
ATP	Adenosine triphosphate
β -TrCP	Beta-transducin repeats containing protein
BCA	Bicinchoninic acid assay
Bcl-2	B-cell lymphoma-2
BH3	Bcl-2 homology domain-3
BHA	Butylated hydroxyanisole
BiP	Binding immunoglobulin protein
BSA	Bovine serum albumin
BSO	L-Buthionine sulfoximine
bZIP	Basic leucine zipper
C/EBP	CCAAT enhancer binding protein

ChaC1	Glutathione Specific Gamma-Glutamylcyclotransferase 1
CHOP	CCAAT-homologous protein
CREB-2	cAMP- response element binding protein 2
CTH	Cystathionine Gamma-Lyase
DA	Dopamine
DAQ	Dopamine quinone
ddH ₂ O	Double distilled water
DIV	Days in vitro
DMSO	Dimethyl sulfoxide
DNA	Deoxyribonucleic acid
dNTP	Deoxyribonucleotide triphosphate
EC-SOD	Extracellular superoxide dismutase
eIF2 α	Eukaryotic initiation factor 2 alpha
eIF5	Eukaryotic initiation factor 5
ER	Endoplasmic reticulum
F2,6P2	Fructose 2,6-bisphosphate
fALS	Familial amyotrophic lateral sclerosis
FCCP	P-trifluoromethoxyphenylhydrazine
GADD34	Growth arrest and DNA damage-inducible protein 34
GADD45 α	Growth arrest and DNA damage-inducible protein 45 alpha

GCL	Glutamylcysteine ligase
GCN2	General control nonderepressible 2
GDP	Guanosine diphosphate
GEF	Guanine nucleotide exchange factor
GFP	Green fluorescent protein
GLU	Glutamate
GLY	Glycine
GOI	Gene of interest
GPx	Glutathione peroxidase
GR	Glutathione reductase
Grp78	78 kDa glucose-regulated protein
GS	Glutathione synthetase
GSH	Reduced glutathione
GSSG	Oxidized glutathione
GTP	Guanosine triphosphate
GST	Glutathione-S-transferase
H ₂ O ₂	Hydrogen peroxide
HBSS	Hanks' balanced salt solution
HIF-PHD	Hypoxia-inducible factor-prolyl hydroxylase domain
HO [•]	Hydroxyl radical

HRI	Heme-regulated eIF2 α kinase
HRP	Horseradish peroxidase
ICH	Intracerebral hemorrhage
ISR	Integrated stress response
ISRIB	Integrated stress response inhibitor
KO	Knockout
LTP	Long term potentiation
MAP2	Microtubule-associated protein 2
MCAo	Middle cerebral artery occlusion
MCB	Monochlorobimane
MEM	Minimum essential media
Met	Methionine
MPP ⁺	1-methyl-4-phenylpyridinium
mRNA	Messenger ribonucleic acid
NADPH	Nicotinamide adenine dinucleotide phosphate hydrogen
NADP ⁺	Nicotinamide adenine dinucleotide phosphate
NAC	N-Acetyl-L-Cysteine
NBM	Neurobasal medium
NO	Nitric oxide
NOX	Nicotinamide adenine dinucleotide phosphate oxidase

NOXA	Phorbol-12-myristate-13-acetate-induced protein 1
nNOS	Neuronal nitric oxide synthase
N-methyl-D-aspartate	N-methyl-D-aspartate
$O_2^{\bullet-}$	Superoxide anion radical
OCR	Oxygen consumption rate
ODDD	Oxygen-dependent degradation domain
ONOO $^{\bullet}$	Peroxynitrite
OXPHOS	Oxidative phosphorylation
PBS	phosphate-buffered saline
PCN	Primary cortical neuron
PCR	Polymerase chain reaction
PD	Parkinson's disease
PERK	Protein Kinase R-like endoplasmic reticulum kinase
PFK2	Phosphofructokinase-2
PFKFB3	6-phosphofructo-2-kinase/fructose-2,6-biphosphatase 3
PHD3	Prolyl hydroxylase domain 3
PIC	Preinitiation complex
PKR	Protein Kinase R
PPP	Pentose phosphate pathway
PUMA	P53-upregulated modulator of apoptosis

qRT-PCR	Quantitative real time polymerase chain reaction
RFU	Relative fluorescent units
RIPA	Radioimmunoprecipitation assay
RNA	Ribonucleic acid
ROS	Reactive oxygen species
SCI	Spinal cord injury
SDS	Sodium dodecyl sulphate
SEM	Standard error of the mean
SIC7A11	Solute Carrier Family 7 Member 11
SN	Substantia nigra
SOD	Superoxide dismutase
TBI	Traumatic brain injury
TBST	Tris buffered saline-tween 20
TC	Ternary complex
TG	Thapsigargin
TH	Tyrosine hydroxylase
Thr	Threonine
Trib3	Tribbles homolog 3
tRNA	Transfer ribonucleic acid
uORF	Upstream open reading frame

UPR	Unfolded protein response
UT	Untreated
WT	Wildtype
Zbtb38	Zinc finger and BTB domain containing 38

Chapter 1

1 Introduction

1.1 Oxidative stress: The balance between free radicals and antioxidants

1.1.1 Free Radical

Oxidative stress is a result of an imbalance between the rate of free radical production and clearance. Free radicals are molecular species with one or more unpaired electrons that are unstable and highly reactive. Some of these are generated due to inefficiencies in biological systems, such as superoxide anion radical ($O_2^{\bullet-}$), which is produced by the leakage of electrons from the electron transport chain during mitochondrial respiration (Cadenas & Davies, 2000). The superoxide anion can dismutate to form hydrogen peroxide (H_2O_2), which cannot react directly with nucleic acids, lipids and most proteins (Halliwell, 2001). In high concentrations however, H_2O_2 can further react through the Fenton reaction to form hydroxyl radical (HO^{\bullet}), which is considered to be the most reactive radical in the body and unlike superoxide, it cannot be eliminated through enzymatic reactions (Bogaerts, Theuns & van Broeckhoven, 2008). The hydroxyl radical can attack purine and pyrimidine bases in DNA, amino acid residues in proteins and it can oxidize lipids, leading to lipid peroxidation (Halliwell, 2001) (Figure 1.1). Other times, free radicals are produced to serve a useful purpose in the cell, such as nitric oxide (NO), which acts as a signalling molecule. NO in the brain is generated by neuronal nitric oxide synthase (nNOS), generally in response to *N*-methyl-D-aspartate (NMDA) receptor activation and contributes to neuronal plasticity (Bredt, 2003). However, during pathological conditions, overactivation of NMDA receptors can lead to excessive production of NO (Girouard et al, 2009). NO can react with superoxide anion radicals to form peroxynitrite ($ONOO^{\bullet}$), a powerful oxidant, which has the ability to damage cellular components such as DNA, lipids and proteins (Halliwell, 2001) (Figure 1.1). There are various processes in the brain that contribute to the production of free radicals. These include the extensive use of glutamate as a neurotransmitter in neurons, auto-oxidation of neurotransmitters such as dopamine as well as the high oxygen consumption of neurons

through the mitochondrial electron transport chain, to keep up with the energy demand of neurons (Halliwell, 2001). Excessive production of free radicals is a contributing factor in the progression and pathogenesis of neurodegenerative diseases. For instance, a decrease in complex I activity of the mitochondria has been shown to be one of the earliest events in the pathogenesis of Parkinson's disease (PD) (Hwang, 2013). Inhibition of complex I leads to increased production of free radicals, which can cause further damage to the mitochondria and other cellular compartments (Halliwell, 2001). Similarly, mitochondrial dysfunction and increased ROS production have been implicated in Alzheimer's disease (AD) (Swerdlow, Burns & Khan, 2015).

1.1.2 Antioxidants

Considering that free radical production happens naturally *in vivo*, there are antioxidant defense systems in place to counterbalance their effects and to prevent damage to cellular components. Antioxidants can be broadly classified into two classes: enzymatic and non-enzymatic.

1.1.2.1 Superoxide dismutases (SODs)

Superoxide dismutases (SODs) are one of the important classes of enzymatic antioxidants that catalyze the dismutation of the superoxide anion into hydrogen peroxide. In eukaryotic cells, there are three forms of SOD (Fattman, Schaefer & Oury, 2003). The first is the copper/zinc SOD (SOD1) that binds both copper and zinc, and is located mainly in the cytosol, nucleus, lysosomes, peroxisomes and the intermembrane space of mitochondria (Valentine, Doucette & Potter, 2005). Mutations in the *sod1* gene account for 20-25% of familial forms of amyotrophic lateral sclerosis (fALS), which makes it the most common cause of inherited ALS (Valentine, Doucette & Potter, 2005). Previous studies have shown that transgenic mice overexpressing Cu/Zn SOD show attenuated neuronal damage following traumatic brain injury (TBI) (Mikawa et al, 1996). Furthermore, it has been shown that reduction in Cu/Zn SOD worsens outcome after transient focal ischemia (Kondo et al, 1997).

The manganese SOD (SOD2) is another important member of this family. As the name suggests, Mn-SOD binds manganese and is found in the mitochondrial matrix. Mice

lacking this enzyme die several days after birth due to severe oxidative damage to the mitochondria in metabolically active cells including cardiomyocytes and neurons (Lebovits et al, 1996).

In addition to intracellular SODs, there is an extracellular SOD (EC-SOD) that is the third member of the SOD family and it is secreted to the extracellular matrix. The role of EC-SOD is not yet fully understood but is thought to prevent formation of peroxynitrite (ONOO^-), which is a toxic product of the reaction between $\text{O}_2^{\cdot-}$ and NO (Fattman, Chaefer, & Oury, 2003). Previous research suggests that mice deficient in EC-SOD develop normally, however, they seem to be more sensitive to hyperoxia (Carlsson, Jonsson, Edlund, & Marklund, 1995) and show a significantly greater volume of cerebral infarct after middle cerebral artery occlusion (MCAo) (Sheng, Brady, Pearlstein, Crapo & Warner, 1999).

SODs are an important part of the antioxidant defense system since they are considered to be the first line of defense against superoxide anions. The final product that is produced by all forms of SODs is H_2O_2 .

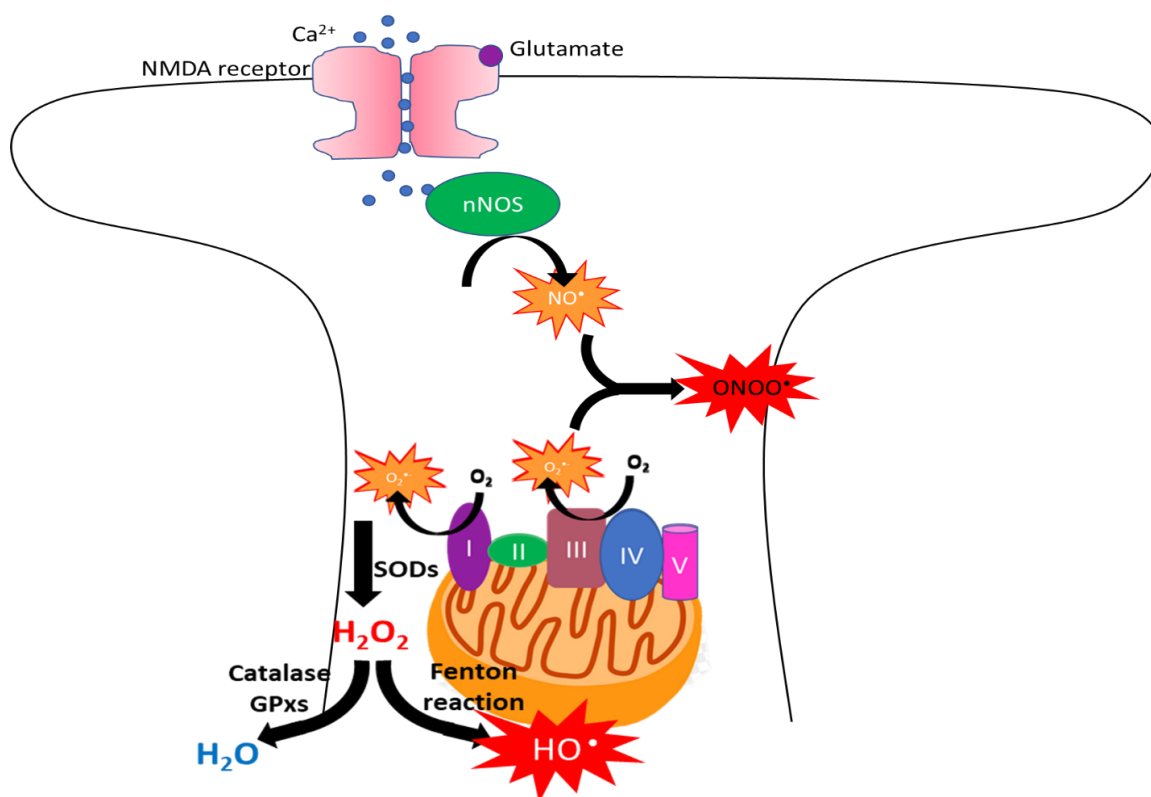


Figure 1.1. Free radical production in neurons. In the process of electron transport in the mitochondria, electrons can leak at complex I and III, allowing them to interact with oxygen (Perier & Villa, 2012). Partial reduction of O_2 leads to the formation of superoxide anion radicals ($\text{O}_2^{\bullet-}$). $\text{O}_2^{\bullet-}$ can react with NO produced by nNOS through the activation of NMDA receptor to form peroxynitrite or can be reduced to hydrogen peroxide by the action of SODs. Hydrogen peroxide can either be reduced to water through the action of catalase or glutathione peroxidase (GPx), or it can form hydroxyl radicals. Both peroxynitrite and hydroxyl radicals are capable of damaging cellular macromolecules.

1.1.2.2 Glutathione system

Hydrogen peroxide can be reduced to water through the enzymatic action of different enzymes including catalase and glutathione peroxidase (GPx). The relative abundance of these two enzymes vary from one tissue to another. For example, GPx activity is higher in the brain compared to catalase, while in the liver both enzymes are equally abundant (Maher, 2005). Furthermore, GPx is present in the mitochondria and is important for reducing H_2O_2 produced in the mitochondria (Maher, 2005). GPxs also function to reduce lipid hydroperoxides to their corresponding alcohols. In humans, GPxs exist in different forms. Among them, GPx1 is the most abundant and the best characterized. GPxs differ based on their localization, as well as their structure and their substrate affinity (Maher, 2005). GPx1 for example, is present in the mitochondria and the cytoplasm of almost all tissues and its preferred substrate is hydrogen peroxide while GPx2 and 3 are highly expressed in the gastrointestinal tract and kidney respectively, with hydrogen peroxide as their preferred substrate as well (Maher, 2005). In contrast, GPx4 has a higher preference for lipid hydroperoxides and is expressed in almost all tissues at a lower level (Yant et al. 2003). Previously, distribution of GPx1 has been mapped in the brain, showing predominant localization in activated microglia and astrocytes (Lindenau, Noack, Asayama & Wolf, 1998). Furthermore, it has been suggested that increased GPx activity modulates recovery of spatial memory after TBI (Tsuru-Aoyagi et al, 2009). GPxs use reduced glutathione (GSH) as a cofactor and an electron donor in the enzymatic reaction of reducing hydrogen and lipid peroxides. Glutathione-S-transferase (GST) is another enzyme whose activity is dependent on a steady supply of GSH. GST acts primarily to detoxify xenobiotics by catalyzing the nucleophilic attack of GSH on electrophilic centers of a wide variety of substrates to prevent them from attacking crucial cell components such as proteins, lipids and nucleic acids (Hayes, Flanagan & Jowsey, 2005). Glutathione itself can also react non-enzymatically (through H transfer) with a wide variety of radicals such as OH^\bullet , OCH_3^\bullet , OOH^\bullet , and is therefore considered to be an excellent free radical scavenger (Galano & Alvarez-Idaboy, 2011). Furthermore, GSH is particularly effective against toxic species such as peroxynitrite and seems to be the only known compound that is capable of scavenging hydroxyl radicals, making it one of the most important antioxidants in the cell (Maher, 2005). In fact, data from primary cortical

neurons show that depletion of GSH sensitizes neurons to oxidative stress-induced cell death (Baxter et al, 2015).

GSH is a tripeptide that is composed of glutamate, glycine and cysteine. Generally, intracellular cysteine level is the limiting factor for synthesis of GSH since glutamate and glycine are present at relatively high concentrations in most cells (Maher, 2005). Evidence from rat primary cortical neurons suggests that addition of N-Acetyl-L-Cysteine (NAC) supplement, which is a precursor for GSH synthesis, to the cultures increases neuronal GSH levels (Dringen & Hamprecht, 1999). Further evidence that points to the importance of cysteine as a rate-limiting precursor for synthesis of GSH comes from a study done in malnourished children, which showed that their low levels of GSH was caused by impaired GSH synthesis that was associated with lower concentrations of cysteine (Reid et al, 2000). A follow up study by the same group later, showed that NAC supplementation increased GSH synthesis rate and concentration (Badaloo, Reid, Forrester, Heird & Jahoor, 2002). The majority of intracellular cysteine comes from reduction of cystine that is imported into the cell by the glutamate/ cystine antiporter, system x_c^- (xCT), which imports one molecule of cystine in exchange for one molecule of glutamate (Maher, 2005). System x_c^- is composed of xCT also known as SIC7A11, the system's light chain, which is the catalytic subunit and confers substrate specificity and 4F2hc, the system's heavy chain, which is the chaperone that recruits SIC7A11 to the plasma membrane (Koppula, Zhang, Shi, Li & Gan, 2017; Maher, 2005). The expression of this transporter in the cells therefore helps in maintaining intracellular GSH levels and protecting cells from oxidative stress by providing the limiting precursor for GSH synthesis (Lim & Donaldson, 2011). Some reports suggest that neurons are unable to take up cystine directly and therefore rely on astrocytes to provide them with GSH precursor, cysteine (Sagara, Miura & Bannai, 1993). This reliance on astrocytes is due to their enhanced ability to take up cystine as a monomer to synthesize GSH. Astrocytes then release large amounts of GSH into the extracellular space, which is broken down, producing glycine and cysteine that can be taken up by neurons (Bélanger, Allaman & Magistretti, 2011). There are other reports however, that suggest that neurons, astrocytes and microglia all express system x_c^- and are capable of importing cystine (Jackman, Uliasz, Hewett & Hewett, 2015). It has been shown that the ectopic expression

of the *SLC7A11*, the key component of system x_c^- , increases GSH biosynthesis in cancer cells (Clemons, Liu, Duong & Phillips, 2017). Once cystine is taken up by the cells, it is reduced to cysteine and can be used as a precursor for biosynthesis of GSH. The thiol group of the cysteine moiety acts as a reducing agent by donating electrons to other molecules such as ROS to neutralize them (Wu, Fang, Yang, Lupton & Turner, 2004).

GSH is synthesized in the cytoplasm in a two-step reaction, each catalyzed by a specific enzyme. The first step is the formation of γ -glutamylcysteine from glutamate and cysteine and is catalyzed by γ -glutamylcysteine ligase (GCL). In the second step, γ -glutamylcysteine then reacts with glycine in a reaction catalyzed by glutathione synthetase (GS) to synthesize GSH (Lu, 2013). It has been shown that the first step of GSH synthesis is the rate limiting step since overexpression of GCL but not GS leads to an increase in GSH levels (Grant, MacIver & Dawes, 1997). Although most of the GSH remains in the cytoplasm, where it was synthesized, some of it is distributed to other organelles such as endoplasmic reticulum (ER), mitochondria and nucleus, where it serves its antioxidant function (Marí, Morales, Colell, García-Ruiz & Fernández-Checa, 2009).

Once GSH reacts either enzymatically or non-enzymatically with free radicals, it is oxidized to GSH disulfide (GSSG), and can only go back to its reduced form by the help of the enzyme glutathione reductase (GR) and NADPH as a reducing agent (Figure 1.2). The main source of NADPH in the cells is the pentose phosphate pathway (PPP), which is an alternative branch of glycolysis (Maher, 2005). Although this pathway does not produce energy in the form of ATP, it is important for producing sugars that are used for synthesizing DNA and RNA and also for producing NADPH, which is essential for regeneration of GSH. It has been shown previously that the rate of glycolysis in neurons is lower than in astrocytes because of the lower activity of PFK2, an enzyme encoded by *pfkfb3* that is responsible for generation of fructose-2,6-bisphosphate (F2,6P2) in neurons (Almeida, Almeida, Bolaños & Moncada, 2001; Almeida, Moncada & Bolaños, 2003). It has also been shown that increasing the rate of glycolysis by overexpressing *pfkfb3* in neurons causes rapid neuronal apoptosis possibly due to a decrease in utilization of glucose through the PPP and consequently, a decrease in regeneration of GSH (Herrero-

Mendez, Almeida, Fernández, Maestre, Moncada & Bolaños, 2009). This suggests that regeneration of GSH from its oxidized form is an important mechanism for keeping the GSH pool in cells. The ratio between GSH and GSSG is an important indicator of the redox status of the cell, with lower ratios being correlated to higher susceptibility of the cells to oxidative stress (Ballatori, Krance, Notenboom, Shi, Tieu & Hammond, 2009).

All these antioxidant defense mechanisms have evolved to protect cells and tissues from free radical attack. There is a controlled balance between the rate of free radical production and its clearance by antioxidants. Any disturbance to this system that causes an imbalance can lead to oxidative stress, which can cause damage to macromolecules and lead to oxidative stress-induced cell death.

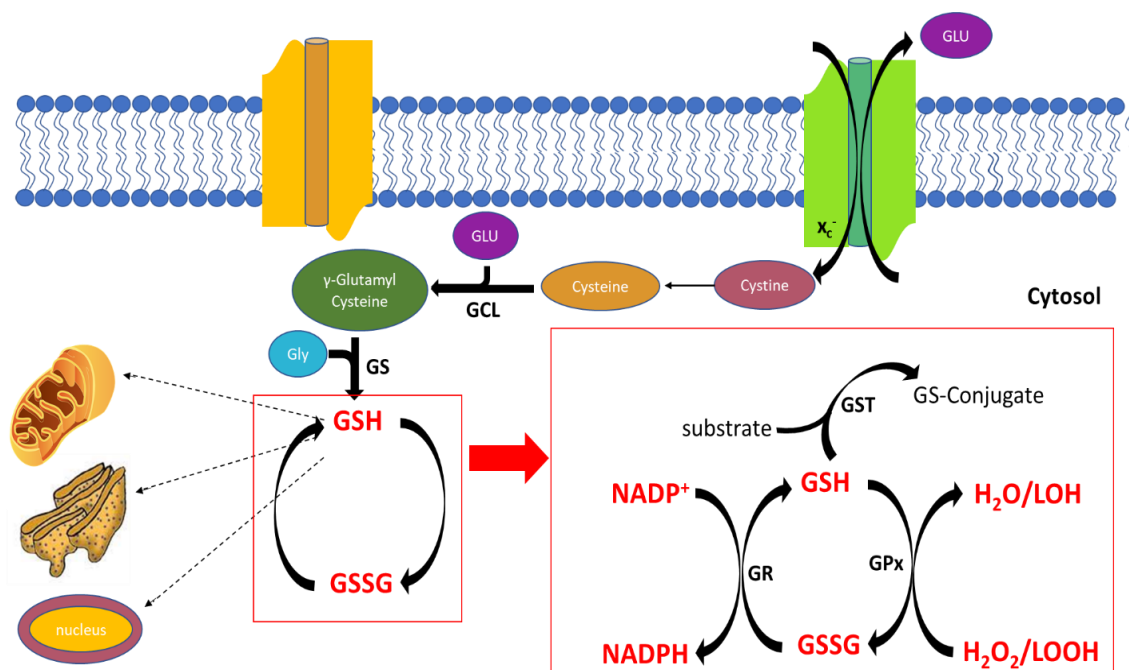


Figure 1.2. Glutathione system. Glutathione is synthesized in a 2-step reaction and is composed of cysteine, glutamate and glycine. Cysteine is the limiting precursor for synthesis of GSH that comes from the reduction of cystine that is imported into the cell by a cystine/glutamate antiporter. The first step of GSH synthesis is the rate limiting step that is catalyzed by enzyme glutamylcysteine ligase (GCL). Once GSH is synthesized in the cytosol, it can be transported to other organelles such as mitochondria, ER and nucleus. GSH can react non-enzymatically with a wide range of ROS in the cell. It can also act as an electron donor in an enzymatic reaction with GPx and GST. Once GSH acts enzymatically or non-enzymatically with free radicals, it is oxidized to GSSG and can only go back to its reduced form with the help of GR and NADPH.

1.2 Oxidative stress and neurodegeneration

Although all tissues can undergo oxidative damage, the brain is particularly susceptible due to its relatively lower enzymatic antioxidant activity, and also due to its high oxygen consumption demand. The brain makes up about 2% of the body weight, but it accounts for 20% of basal oxygen consumption (Uttara, Singh, Zamboni & Mahajan, 2009). This high demand for oxygen is to meet the metabolic needs of neurons in terms of ATP production required for signaling and action potential propagation. This also means that in order to meet this high energy demand, mitochondrial activity is of utmost importance in these cells. One consequence of high levels of mitochondrial respiration is an increase in the rate of free radical production by the mitochondria. Furthermore, with glutamate being the most abundant excitatory neurotransmitter in the brain, there is an increased rate of NO production due to activation of nNOS. In addition to this, resident microglia in the brain generate free radical species such as O_2^- , H_2O_2 and NO (Halliwell, 2001). Additionally, the fact that neurons are post-mitotic and cannot regenerate themselves makes them susceptible to oxidative stress-induced neurodegeneration due to accumulation of oxidative damage over time.

1.2.1 Aging and oxidative damage

An increase in mitochondrial dysfunction and oxidative damage has been seen in aging and age-related neurodegenerative diseases (Cassarino, & Bennett, 1999). Aging has long been correlated with the accumulation of oxidative damage to cellular macromolecules. Numerous studies have shown that levels of DNA damage (both mitochondrial and nuclear) and lipid peroxidation are increased with aging (Liu & Xu, 2011). The accumulation of oxidative damage over years can also modify the activity and structure of certain proteins, causing a variety of age-related diseases (Ethen, Reilly, Feng, Olsen & Ferrington, 2007; Machado, Ayala, Gordillo, Revilla & Santa Maria, 1991). Oxidative damage has been shown to increase with age in various organisms including mice, flies and C-elegans (Liu & Xu, 2011). Various animal and human studies

suggest that GSH concentration declines with age, largely because of diminished supply of its precursors such as cysteine (Sekhar et al, 2011). Furthermore, data from *Drosophila melanogaster* suggests that NAC supplementation slows down aging and increases lifespan (Brack, Bechter-Thüring & Labuhn, 1997). Considering that oxidative damage is an important factor in aging, it is not surprising to see it as a hallmark of various age related neurodegenerative diseases such as Alzheimer's disease (AD) and Parkinson's disease (PD).

1.2.2 Alzheimer's disease

Alzheimer's disease is a progressive neurodegenerative disorder and is the most common form of dementia, affecting predominantly individuals over the age of 65. Although different risk factors have been identified for this disease, aging remains the most important. AD is characterized by aggregation of extracellular amyloid plaques and intracellular neurofibrillary tangles (Tönnies, & Trushina, 2017). However, the underlying cause of the disease remains to be elucidated. There are various hypotheses regarding the disease mechanism and progression, which suggest that oxidative stress could either be the cause or the consequence of A β deposition (Du, Wang & Geng, 2018). Many studies have shown that protein oxidation and lipid peroxidation are increased in the brains of patients with AD (Hensley et al, 1995; Palmer & Burns, 1994; Marcus et al, 1998). Additionally, peroxynitrite, a potent oxidant that is formed by the reaction of superoxide with nitric oxide, is elevated in brains of AD patients, specifically, within the neurofibrillary tangles, further highlighting the importance of oxidative stress in the pathology of AD (Good, Werner, Hsu, Olanow & Perl, 1996; Smith, Richey Harris, Sayre, Beckman & Perry, 1997). Lipid peroxidation has also been shown to be the major cause of membrane phospholipid depletion in AD (Prasad, Lovell, Yatin, Dhillon & Markesbery, 1998). Clinically, GSH measurement using magnetic resonance spectroscopy in AD patients and healthy controls has shown GSH levels to be significantly decreased in both males and females with AD (Mandal, Tripathi & Sugunan, 2012). Furthermore, both *in vivo* and *in vitro* studies in mice report an AD-associated GSH decrease, suggesting that the increase in the ROS level is partly due to a decrease in the level of antioxidants (Resende et al, 2008; Ghosh, LeVault, Barnett & Brewer, 2012).

Post mortem brain tissues from AD patients also show that there is a decrease in GSH/GSSG ratio (Ansari & Scheff, 2010). Interestingly, the reduction of cellular GSH/GSSG ratio is shown to correlate with the activation of caspases and the loss of anti-apoptotic protein Bcl2 (Filomeni, Rotilio & Ciriolo, 2003). There is a great body of research investigating the therapeutic potential of antioxidants in AD. One example is NAC that has been investigated as a potential therapeutic agent. NAC is also able to protect against A β induced protein oxidation and lipid peroxidation. Furthermore, it can enhance the activity of GPx and GR that has been diminished in APP/PS-1 knock-in mice (Huang et al, 2010). These data highlight the role of oxidative stress in the progression of AD as well as the role of antioxidant defense in delaying and ameliorating AD symptoms.

1.2.3 Parkinson's disease

Another neurodegenerative disease that is associated with oxidative stress is Parkinson's disease (PD). PD is characterized by the selective loss of dopaminergic (DA) neurons of the substantia nigra (SN) and abnormal aggregation of alpha-synuclein protein known as Lewy bodies (Hauser & Hastings, 2013). Both *in vivo* and *in vitro* models of PD report mitochondrial dysfunction, specifically, a decrease in complex I activity, to be one of the earliest events in the pathogenesis of the disease (Hwang, 2013). Previous studies have shown that drugs such as MPP⁺ and Rotenone inhibit complex I of the mitochondrial respiratory chain and cause an increase in the amount of superoxide produced by complex I (Langston, Forno, Rebert & Irwin, 1984; Betarbet, Sherer, MacKenzie, Garcia-Osuna, Panov & Greenamyre, 2000). Blocking mitochondrial complex I using rotenone in mice caused selective degeneration of nigrostriatal dopaminergic neurons that was accompanied by behavioral and neurological features of PD (Betarbet et al, 2000). Recent work suggests that one of the reasons why nigral DA neurons are highly vulnerable in PD is due to their specific morphological and bioenergetic characteristics. These data suggest that this particular population of neurons has a higher rate of mitochondrial oxidative phosphorylation (OXPHOS) and a higher density of axonal mitochondria as well as

increased basal level of oxidative stress, all due to their highly complex axonal arborization (Pacelli, Giguère, Bourque, Lévesque, Slack & Trudeau, 2015). The mitochondrial dysfunction alone however, does not explain the selective degeneration of the specific cell types in the SN. Another factor that may play a role in increasing the vulnerability of these cells to oxidative stress is the metabolism of DA itself. Although DA is usually stored in vesicles, excess cytosolic dopamine can be oxidized to form dopamine quinones (DAQ) (Hwang, 2013). DAQs can covalently react with low molecular weight thiols such as GSH and protein cysteinyl residues, which can have adverse effects on cellular function and health (Hauser & Hastings, 2013). Additionally, DAQs can also make highly reactive species known as aminochromes that can generate superoxide anions and deplete cellular NADPH, the essential precursor for regeneration of GSH (Hwang, 2013). Post mortem analyses have shown that there is a significant loss of GSH and a decrease in GSH/GSSG ratio in the substantia nigra of patients with PD (Dexter et al, 1994; Sian et al, 1994). Although this is not thought to be the cause of PD, it is considered to be an early event in the progression of the disease, which makes cells more susceptible to ROS attack and oxidative damage (Jenner, 1994).

1.2.4 Stroke

Increases in ROS and oxidative stress have also been seen in conditions such as ischemic stroke (Chan, 2001). The neuronal damage caused by ischemia is due to interruption of blood flow, hypoxia, ATP depletion and the reperfusion that follows. Under hypoxic conditions, oxygen is depleted and the cell switches to glycolysis where ATP can be produced anaerobically. In this pathway, lactate and H^+ accumulate in the mitochondria and result in acidosis. Acidosis contributes to ROS formation since H^+ can enhance the conversion of $O_2^{\cdot -}$ to H_2O_2 and consequently HO^{\cdot} (Shirley, Ord & Work, 2014). Reperfusion has also been shown to have deleterious effects on the brain since it causes a rapid increase in ROS production by the mitochondria (Chouchani et al, 2015). NADPH oxidase (NOX) is one of the enzymes that is thought to be the main source of ROS production after ischemia/reperfusion injury (McCann, Dusting & Roulston, 2008). Previous studies have shown that inhibition of NOX reduces the oxidative stress and infarct volume as well as the post-ischemic inflammation in the brain (Chen, Song &

Chan, 2009; Chen, Kim, Okami, Narasimhan & Chan, 2011). Different strategies have been explored to lower ROS levels after stroke in order to manage and reduce the extent of injury. Free radical scavengers such as lipoic acid and NAC have shown promising results by reducing lesion volume significantly (Clark, Rinker, Lessov, Lowery & Cipolla, 2001; Khan et al, 2004). In fact, several compounds with antioxidant capacity have been developed, some of which progressed to clinical trials and even to the market. For example, Edaravone is a free radical scavenger that showed promising results in rats with focal ischemia and is now used in some countries as a therapy for stroke recovery (Amemiya et al, 2005; Miyaji et al, 2015). These results highlight the importance of ROS production in pathogenesis of ischemic stroke and reperfusion.

Overall, it has been well established that disruption of the homeostatic balance between the production and clearance of free radicals in the brain can sensitize neurons to oxidative stress and have irreversible consequences. Considering the post-mitotic nature of neurons, prompt and efficient action of antioxidants is therefore of utmost importance for the survival of these cells. Despite the knowledge about the involvement of oxidative damage in different neurodegenerative diseases the mechanisms underlying antioxidant depletion is not fully understood.

1.3 The role of integrated stress response during cellular stress

The integrated stress response (ISR) is an evolutionarily conserved adaptive pathway that is activated in response to cellular stress and acts to ameliorate the disturbance and restore homeostasis. In addition to oxidative stress, there are various stressors that can activate the ISR pathway including amino acid deprivation, endoplasmic reticulum (ER) stress, hypoxia, heme deprivation, viral infection, etc. Each of these stressors may activate one or more of the four different kinases involved in the ISR: GCN2, PKR, HRI and PERK. Activation of each of these kinases leads to phosphorylation of the alpha subunit of the eukaryotic initiation factor 2, eIF2 α (Pakos-Zebrucka, Koryga, Mnich, Ljubic, Samali & Gorman, 2016). eIF2 is a heterotrimer that is composed of an alpha, a beta and a gamma subunit (Kimball, 1999). Phosphorylation of eIF2 α under stress

condition leads to general inhibition of protein translation, which acts to conserve energy and nutrients and to provide a temporary relief from the stress (Harding, Zhang, Bertolotti, Zeng & Ron, 2000; Lu et al, 2004). Under normal conditions, GTP-bound eIF2 binds to tRNA carrying the first amino acid, methionine (Met-tRNA_i), forming the ternary complex (TC). The TC then binds to the 40S ribosomal subunit, creating the 43S preinitiation complex (PIC). The PIC then binds to the mRNA that has already been unwound and starts searching along the mRNA for the start codon, AUG. Once AUG is paired with methionine, eIF5, which is a GTPase-activating protein is recruited to the complex, and it induces GTP to be hydrolyzed to GDP. This hydrolysis allows for the 40S ribosomal subunit to be dissociated from the complex, bind to the 60S ribosomal subunit and initiate the protein translation. The GDP bound to eIF2 then needs to be exchanged for GTP to allow for another round of translation initiation, and this is done with the help of the guanine nucleotide exchange factor (GEF), eIF2B (Sonenberg & Hinnebusch, 2009). Figure 1.3 shows the schematic of translation initiation and the important players involved in the process. eIF2B has 5 different subunits, 2 of which are catalytic and the other 3 are regulatory subunits (Sidrauski et al, 2015). Once eIF2 α is phosphorylated during stress conditions, its binding affinity for eIF2B increases and so acts as an inhibitor of the GEF (Krishnamoorthy, Pavitt, Zhang, Dever & Hinnebusch, 2001). Since the cellular concentration of eIF2B is much lower than eIF2, its activity can be abolished even by a small amount of eIF2 phosphorylation. The inhibition of eIF2B renders the cell unable to re-initiate protein translation leading to a significant attenuation in the general protein synthesis, which acts to protect cells during acute stress (Sidrauski et al, 2015). Interestingly, there are certain proteins that are preferentially translated during this process, such as Activating Transcription Factor 4 (ATF4).

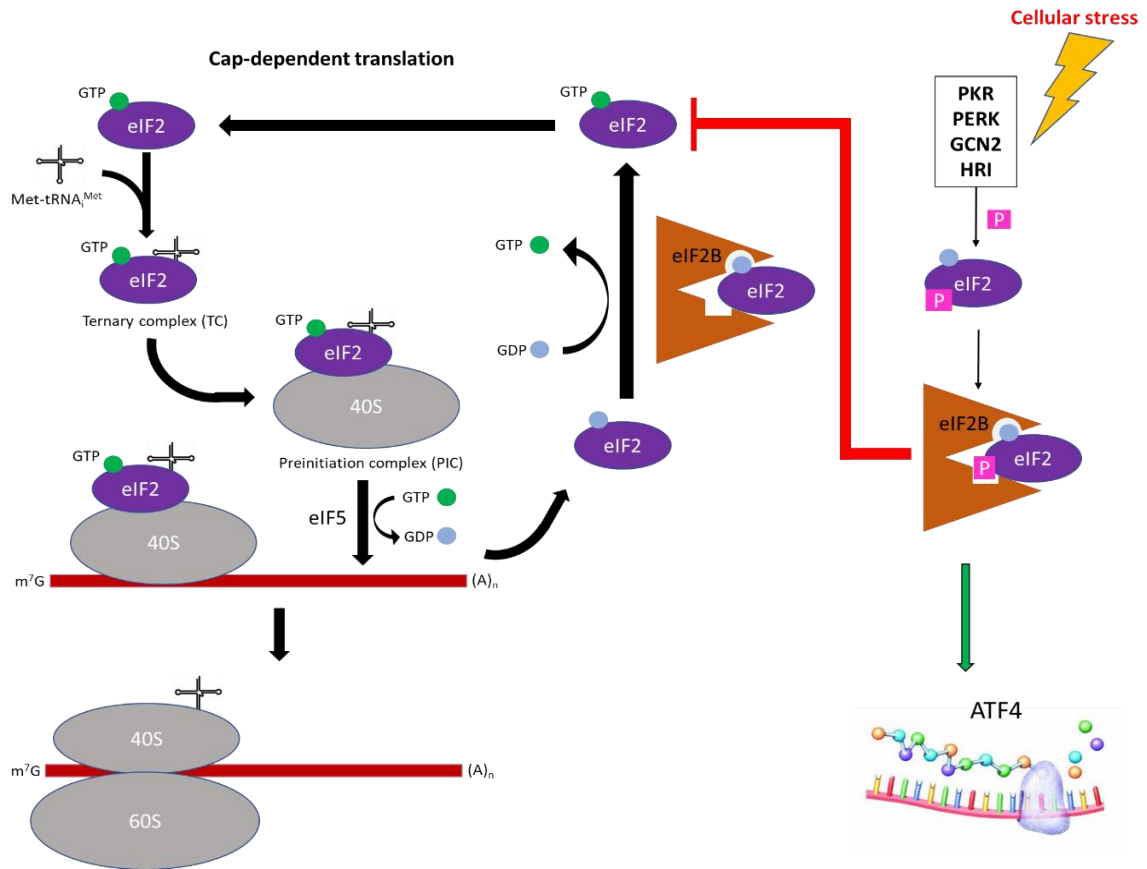


Figure 1.3. Integrated stress response (ISR) regulates translation initiation and allows for translation of ATF4. Under normal conditions, GTP-bound eIF2 binds to tRNA carrying methionine and forms the ternary complex (TC). The TC then binds to the 40S ribosomal subunit and creates the preinitiation complex (PIC). PIC binds to the mRNA and starts scanning through the length of it to find the start codon, AUG. Once methionine is paired with AUG, eIF5 is recruited to hydrolyze GTP to GDP and allow the dissociation of the complex from the 40S ribosomal subunit. The 40S ribosomal subunit can then bind to 60S subunit and initiate translation initiation. In order for another round of translation initiation to begin, the GDP bound to eIF2 needs to be exchanged for GTP, and this is done with the help of guanine nucleotide exchange factor, called eIF2B. eIF2B has a higher affinity for phosphorylated eIF2. Therefore, under stress conditions when the alpha subunit of eIF2 is phosphorylated by different kinases, it acts as an inhibitor of eIF2B, rendering the cell unable to reinitiate protein synthesis, leading to inhibition of general protein translation. During this process, certain proteins such as ATF4 are preferentially translated.

1.3.1 Activating Transcription Factor 4

ATF4, also known as cAMP- response element binding protein 2 (CREB-2) is a basic leucine zipper (bZIP) transcription factor, which can homo- or heterodimerize with other bZIP transcription factors through the leucine zipper region. The basic region is upstream of the leucine zipper, which contains positively charged amino acids that function as the DNA-binding domain (Vallejo, Ron, Miller & Habener, 1993; Karpinski, Morle, Huggenvik, Uhler, & Leiden, 1992). ATF4 can homo- or heterodimerize with other bZIP transcription factors, which includes three major subfamilies: cJun/cFos, ATF/CREB and CCAAT enhancer binding protein (C/EBP) (Wortel, van der Meer, Killberg & van Leeuwen, 2017). ATF4 also has other functional domains including the N-terminal domain, which contains a p300 interaction site. P300 is a histone acetyltransferase that acts as a transcriptional coactivator, by binding to transcription factors and regulating transcription initiation (Teufel, Freund, Bycroft & Fersht, 2007). It has been shown that p300 allows for stabilization of ATF4 by inhibiting ubiquitination and proteasomal degradation of the protein, which is independent of its acetyltransferase activity (Lassot, Estrabaud, Emiliani, Benkirane, Benarouse & Margottin-Goguet, 2005). Other domains/motifs that are present on the ATF4 protein and affect its stability are an oxygen-dependent degradation domain that is recognized by PHD3 and a β -TrCP recognition motif, which is targeted for proteasomal degradation (Figure 1.4) (Scortegagna et al, 2014; Lassot et al, 2001). ATF4 exists as a monomer in the absence of a DNA target. In the presence of a DNA target, it can form homodimers on the DNA that are of low relative stability (Podust, Krezel & Kim, 2000). On the other hand, ATF4 can also form heterodimers, which are more stable and bind to the DNA with higher affinity (Podust, Krezel & Kim, 2000). This protein is an integral part of the ISR and acts as an effector element by transcriptionally regulating the expression of different genes. The main hypothesis regarding the expression of ATF4 protein is that the *ATF4* mRNA is preferentially translated in response to eIF2 α phosphorylation because of the contribution of the two upstream open reading frames (uORFs) in the 5' region of its mRNA. Normally, once the proximal uORF (uORF1) has been translated, GDP is exchanged for GTP, allowing the eIF2-TC complex to be reacquired and the translation to be reinitiated

at uORF2. The second uORF is inhibitory, thereby reducing the expression of ATF4 protein. Under stress conditions where eIF2-GTP levels are low, translation initiation is delayed, causing the 40S ribosome to scan through the inhibitory subunit, allowing ATF4 to be expressed (Vattem & Wek, 2004).

Although ATF4 is expressed in many cell types and is an important part of the cells' stress response, its role in the embryonic development and differentiation of osteoblasts has also been investigated thoroughly. Consequently, it has been found that ATF4-deficient mice tend to have delayed bone formation and a reduced bone mass (Yang et al, 2004). ATF4 deficiency also causes microphthalmia, highlighting the importance of the protein in the formation of lens fibres and the anterior lens epithelial cells during development (Tanaka et al, 1998; Hettmann, Barton & Leiden, 2000).

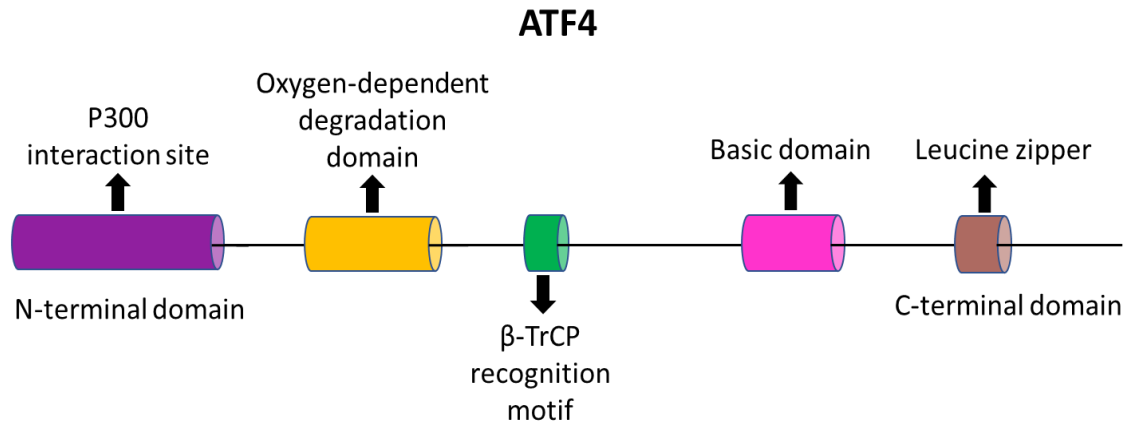


Figure 1.4. Functional domains of ATF4 protein. ATF4 protein has a leucine zipper domain on its C-terminal end, which is essential for heterodimerization with other bZIP transcription factors. Upstream of the leucine zipper, there is a basic domain that is important for DNA binding. There is also a β -TrCP recognition motif that is dependent on the phosphorylation events on ATF4. β -TrCP recognizes specific phosphorylated residues and targets the protein for proteasomal degradation. ATF4 protein stability is also affected by the oxygen-dependent degradation domain (ODDD), which is recognized by PHD3. Finally, there is a p300 interaction site at the N-terminal domain of the protein. P300 stabilized ATF4 protein by inhibiting ubiquitination and proteasomal degradation.

During stress conditions, ATF4 seems to play a dual role depending on the target genes it induces (Wortel, van der Meer, Killberg & van Leeuwen, 2017). ATF4 can translocate into the nucleus and regulate the expression of adaptive genes that are involved in amino acid transport and metabolism, oxidative stress and protein homeostasis to help relieve the stress (Harding et al, 2003). For example, ATF4 induces GADD34, which is important for initiating a negative feedback loop, dephosphorylating eIF2 α and restoring protein translation (Ma & Hendershot, 2003). It can also induce genes that are important for cell survival such as Grp78/BiP, which encode ER chaperone proteins to enhance protein folding (Luo, Baumeister, Yang, Abcouwer & Lee, 2003). However, if the stress condition persists, and ATF4 upregulation is sustained, it can induce apoptosis and cell-cycle arrest through the induction of pro-apoptotic genes such as CHOP (Zinszner et al, 1998; Galehdar, Swan, Fuerth, Callaghan, Park & Cregan, 2010). In addition to the duration of stress, the effects of ATF4 seem to be cell type-dependent. In fibroblasts for instance, it has been shown that ATF4 deficient cells are impaired in activating genes that are important for protection against oxidative stress, while ATF4 deficient neurons seem to be protected against oxidative stress (Harding et al, 2003; Lange et al, 2008). This may be because certain pro-death genes such as Trib3 are induced by ATF4 under stress conditions in neurons but not in fibroblasts (Lange et al, 2008). Most of the literature in non-neuronal cells tends to emphasize the pro-survival role of ATF4, however, it is generally accepted that sustained activation of ATF4 can be detrimental for most cells. Another factor that may modulate specific gene transcription and affect the signalling outcome is the formation of heterodimers with different bZIP family members by ATF4. For example, interaction with ATF3 and CHOP has been shown to activate NOXA, a Bcl-2 homology3 (BH3)-only pro-apoptotic protein and Trib3, respectively (Wang et al, 2009; Ohoka, Yoshii, Hattori, Onozaki & Hayashi, 2005). On the other hand, interaction with C/EBP γ is important for expression of stress-induced genes such as *ChaC1*, *SIC7A11*, *ASNS* and *CTH*, which are involved in oxidative homeostasis and amino acid biosynthesis and transport (Huggins et al, 2015). The effect of ATF4 activation is therefore highly context dependent. ATF4 can also undergo various post-translational modifications, which can affect the stability as well as the transcriptional activity of the protein. For instance, post-translational stabilization, using the proteasome inhibitor

MG132 has been shown to be an effective method for expression of ATF4 protein (Milani et al, 2009). Other examples of post-translational modifications include phosphorylation of ATF4 at specific threonine residues (Thr107, Thr114, Thr5, Thr119), which destabilizes the protein and inhibits its transcriptional activation of PUMA and NOXA, both of which are important mediators of the pro-apoptotic response (Bagheri-Yarmand et al, 2015). Additionally, methylation of ATF4 on arginine residue 239 has been shown to modulate its transcriptional properties (Yuniati et al, 2016).

1.3.2 The role of ISR and ATF4 expression in neurons

The role of ISR and ATF4 expression has been investigated in various neurodegenerative diseases as well as hypoxia, TBI and spinal cord injury.

1.3.2.1 Alzheimer's disease

Mounting evidence suggests that the ISR is activated in both *in vivo* and *in vitro* models of AD. Previously it has been shown that p-eIF2 α is elevated in the hippocampus and the prefrontal cortex in the APP/PS1 AD mouse model (Ma et al, 2013). These results have also been confirmed by immunohistochemical studies of post mortem AD brains compared to their age-matched controls. In these studies, eIF2 α staining was shown to be elevated in the cell bodies of hippocampal neurons of AD brains as compared to age-matched control brains (Chang, Wong, Ng & Hugon, 2002). It has also been shown that treatment of rats' primary cortical and hippocampal neurons with A β oligomer *in vitro* increases Trib3 mRNA and protein levels, which is a pro-apoptotic transcriptional target of ATF4 (Saleem & Biswas, 2016). These results were also confirmed *in vivo* by injecting A β oligomer directly into rat brain. Consequently, oligomeric A β has been shown to induce apoptosis both *in vitro* and *in vivo* (Saleem & Biswas, 2016). Deletion of *PERK*, an eIF2 α kinase that has been implicated in AD, prevented A β -induced impairments in LTP as well as other AD associated abnormalities such as spatial memory deficits (Ma et al, 2013). But PERK does not seem to be the only eIF2 α kinase that has been associated with AD. Immunohistochemical staining has shown that the AD brains also have a higher level of phosphorylated PKR in the degenerating neurons

(Chang, Wong, Ng & Hugon, 2002). Cellular models of AD have shown that ATF4 is synthesized axonally in response to A β treatment, which is in turn important for the retrograde transport and A β -induced neurodegeneration (Baleriola et al, 2014). Interestingly, recent data suggests that treating neurons with ISRIB, which has been shown to restore protein translation downstream of eIF2 α , protect cells from A β -induced neuronal cell death (Halliday et al, 2015; Hosoi, Kakimoto, Tanaka, Nomura & Ozawa, 2016).

1.3.2.2 Parkinson's disease

Evidence suggests that in various cellular models of PD, such as the 6-OHDA and MPP⁺ paradigms, ER stress is induced, causing upregulation of ATF4 and CHOP expression (Ryu, Harding, Angelastro, Vitolo, Ron & Greene, 2002). It has also been shown that overexpression of ATF4 in rat SN *in vivo* significantly increases caspase 3/7 activity and reduces the percentage of tyrosine hydroxylase (TH)-positive cells (Gully et al, 2016). Moreover, the pro-apoptotic gene, Trib3, has been shown to be highly induced in response to 6-OHDA and MPP⁺ treatments in PC12 neuronal cells and that upregulation of Trib3 in PD paradigms promotes cell death (Rye, Angelastro & Greene, 2005; Aimé et al, 2015). Interestingly, Trib3 upregulation has also been observed in SN dopaminergic neurons in post-mortem tissue from human PD patients (Aimé et al, 2015).

1.3.2.3 Stroke and spinal cord injury

The role of ATF4 has also been investigated in models of ischemic and hemorrhagic stroke. In a study conducted by Lange and colleagues, it was demonstrated that ATF4 deficient mice are less susceptible to ischemic brain damage, showing smaller infarct volumes and faster recovery after transient middle cerebral artery occlusion (MCAo) a model of ischemia-reperfusion injury (Lange et al, 2008). Interestingly, in another study published by the same group, it was shown that intraperitoneal administration of adaptaquin, a HIF-PHD inhibitor, in rats, prevented neuronal death in an intracerebral hemorrhage (ICH) stroke model and this was attributed to the suppression of ATF4 mediated expression of pro-death genes (Karuppagounder et al, 2016). Involvement of

ATF4 has also been implicated in spinal cord injury (SCI). Evidence for this comes from a study which suggests that ATF4 binds directly to the promoter of the gene *Zbtb38/CIBZ*, which is involved in SCI (Cai et al, 2017; Cai, Li, Yang, Li, Zhang & Liu, 2012). Furthermore, knockdown of ATF4 caused a decrease in the expression level of *Zbtb38* (Cai et al, 2017).

The involvement of ATF4 in neuronal apoptosis has also been investigated in cell-based models. ATF4 induction using the ER-stressor, thapsigargin, causes cell death through upregulation of PUMA, which is mediated by the induction of its proapoptotic target gene, CHOP (Galehdar et al, 2010). Cell-based models also show that restoration of protein synthesis downstream of eIF2 α through treatment with ISRIB leads to a reduction in neurodegeneration induced by pathogenic prion protein in rats (Halliday et al, 2015). Moreover, previous data suggest that ectopic overexpression of ATF4 in primary cortical neurons causes a reduction in GSH levels and a consequent decrease in cell viability, which can be mitigated by the addition of other antioxidants such as butylated hydroxyanisole (BHA) (Lange et al, 2008).

1.4 Rationale

ATF4 is a stress-inducible protein that is upregulated in response to a variety of cellular stressors including ER-stress and oxidative stress. There have been various reports that have shown elevation of factors both upstream and downstream of ATF4, such as eIF2 α phosphorylation and Trib3 induction in *in vitro* and *in vivo* models of AD and PD. We and others have demonstrated that prolonged activation of ATF4 promotes neuronal cell death, however, the mechanism behind it remains unclear. The importance of GSH as an antioxidant has been highlighted in other studies where its depletion has been shown to sensitize neurons to oxidative stress-induced cell death. Previously it was suggested that ectopic overexpression of ATF4 in primary cortical neurons leads to GSH depletion and neuronal cell death, which can be mitigated through the addition of antioxidants to the culture. However, it remains unclear whether upregulation of endogenous ATF4 affects glutathione levels during neuronal stress.

1.5 Hypothesis

Upregulation of endogenous ATF4 through the conventional pathway of ISR activation, depletes cellular GSH and sensitizes neurons to oxidative stress-induced cell death (Figure 1.5).

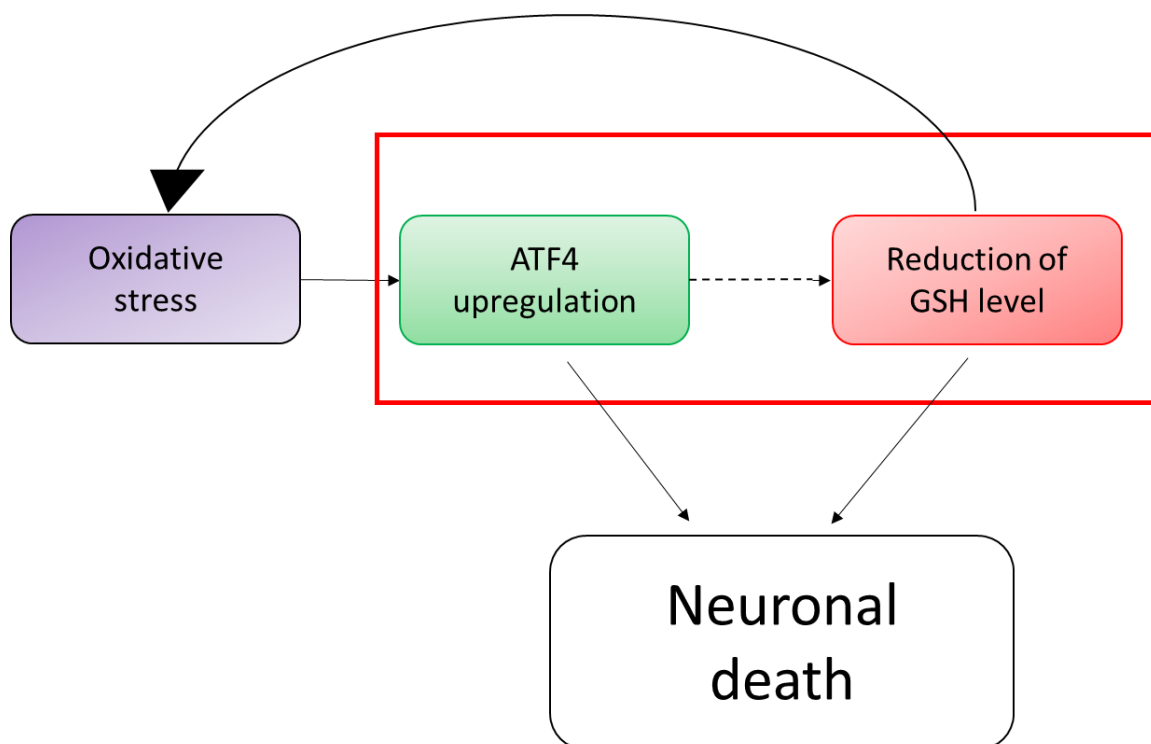


Figure 1.5. Rationale and hypothesis. Oxidative stress conditions can induce neuronal apoptosis through the induction of ISR and upregulation of ATF4. Glutathione depletion, which contributes to oxidative stress can also induce neuronal death. Recent evidence suggests that ATF4 might not only be the consequence of GSH depletion and oxidative stress but can even be a cause of it since its ectopic overexpression has shown to decrease GSH levels in neurons. In this project, we investigated the effect of endogenous ATF4 upregulation on neuronal GSH levels, in order to establish a relationship between the two.

Chapter 2

2 Materials and Methods

2.1 Animals

All animal procedures were carried out according to the protocols approved by the Animal Care Committee at University of Western Ontario. Mice carrying an ATF4-null mutation were obtained from Drs. Tim Townes and Joe Sun (University of Alabama at Birmingham, AL) (Masuoka & Townes, 2002). Wildtype and knockout littermates used for experimentation were generated by breeding heterozygous mice.

2.1.1 Genotyping

Genomic DNA was isolated using phenol/chloroform/isoamyl alcohol (Fisher Bioreagents®, FL-06-0205). The wildtype allele was detected using the primer 5'-AGCAAAACAAGACAGCAGCCACTA-3', and the common reverse primer 5'-GTTTCTACAGCTTCCTCCACTCTT-3'. The ATF4-knockout allele was detected using the primer 5'-ATATTGCTGAAGAGCTTGGCGGC-3'. PCR reagents (Taq polymerase, 10x buffer, 50 mM MgCl₂, and Q Solution) were purchased from Qiagen (Toronto, ON - 201205). The dNTPs were purchased from Life Technologies (Burlington ON - 10297-018). The PCR cycling conditions were programmed as such: initial PCR activation step (95°C, 2 min), cycling step (denaturation 94°C, 20 sec; annealing 62°C, 30 sec; elongation 68°C, 90 sec, x 30 cycles), followed by a final extension step (70°C, 10 mins). The samples were then cooled at 4°C.

2.2 Cell culture

2.2.1 Primary cortical neurons

Primary neuronal cultures were dissected from the cerebral cortices of embryonic mice day 14.5-15.5 (E14.5-15.5). Pregnant mice were euthanized with 700 mg/kg of sodium pentobarbital, injected intra-peritoneally prior to cervical dislocation. The cortices from

each embryo was stored and processed separately after the removal of the meninges. A tail sample of each embryo was also obtained separately for genotyping purposes.

Immediately after dissection, the cortices were placed in 1×Hanks' Balanced Salt Solution (HBSS; Gibco®, 14170-112) and kept on ice until processing time. To dissociate the cortical tissue, individual cortices were trypsinized with 1×HBSS solution supplemented with 1×trypsin (Sigma, T4549) as well as 1.2 mM MgSO₄ and were placed in a 37°C incubator for 25 minutes. The trypsin was then inhibited by the addition of 600 µL of 1×HBSS supplemented with 1.2 mM MgSO₄, 0.2 mg/mL trypsin inhibitor (Roche, 10109878001) and 0.25 mg/mL DNase I. The samples were mixed thoroughly and centrifuged for 4 minutes at 400×g. After the centrifugation, the supernatant was removed, and the pellet was resuspended in 1 mL of 1×HBSS solution supplemented with 3 mM MgSO₄, 0.8 mg/mL DNase I and 1.25 mg/mL trypsin inhibitor. To further dissociate the tissue, the pellets were triturated 10-15 times with a flame polished pipette. The samples were centrifuged one last time to pellet the cells and were resuspended in 2 mL of complete neurobasal media (NBM; Gibco®, 21103-049) supplemented with 0.5×B27 (Life Technologies, 17504044), 1×N2 (Life Technologies, 17502048), 0.5×Glutamax (Life Technologies, 35050061) and 50 U/mL penicillin: 50 µg/mL streptomycin (Life Technologies, 15140-122).

The cell suspension was diluted in supplemented NBM to a concentration of 6×10^5 cells/mL and plated in either 35mm (2 mL; 1.2×10^6 cells/dish) or 4-well (500 µL; 3×10^5 cells/well) dishes. The dishes (NunclonΔ Surface, Thermo Scientific) were pre-coated with poly-L-ornithine (Sigma, P4957) (diluted 1:10 in ddH₂O) over night and rinsed with ddH₂O. Cultures were maintained in a 37°C incubator with 5% CO₂ until ready for use.

2.2.2 N2A Cell line

N2A cells were used for overexpression experiments. The mouse neuroblastoma cell line was purchased from ATCC® (CCL-131™). Cells were maintained in complete growth media made up of 90% Minimum Essential Media (MEM; Gibco®, 11095-080), 10% Fetal Bovine Serum (FBS; Gibco®, A31607-01), 0.5% 50 U/mL penicillin: 50 µg/mL streptomycin and 0.02% Gentamicin (Sigma, G1272). Cells were grown in T75 flasks

(Thermo Scientific) and were passaged every 5 days at 1:50 dilution. For experiments, N2A cells were plated at 2×10^5 cells/well density in 6-well plates (Cellstar®, 657160) and were incubated at 37°C with 5% CO₂ overnight, to allow adherence to the bottom of the plate.

2.2.3 Plasmid transfection

Lipofectamine®2000 (Invitrogen, 11668-019) was used to transfect the N2A cells with 2µg of the pGFP or pcDNA3-mATF4. The plasmids were first diluted to 0.1 µg/µl in DNase/RNase-free water. Plasmids (2µg) were then diluted in 180 µl of 1×Opti-MEM (Gibco®, 31985-070), bringing the volume to 200 µl. Lipofectamine was also diluted in 1×Opti-MEM (4µl of lipofectamine in 200 µl of 1×Opti-MEM). The diluted lipofectamine was then mixed with diluted plasmid and incubated at room temperature for 30 minutes before being added to the cells. The transfection media stayed on the cells for 30-36 hours before the cells were harvested for RNA and protein.

2.2.4 Drugs

ER-stress was induced using Thapsigargin (TG) (T9033, Sigma). Stock was made by solubilizing the contents in DMSO to a concentration of 1mM. L-Buthionine sulfoximine (BSO) (B2515, Sigma) stocks were made in DMSO at 100mM concentration. Antioxidants N-Acetylcysteine (NAC) (A7250, Sigma) and Butylated hydroxyanisole (BHA) (B1253, Sigma) stocks were made in DMSO and ethanol at 200mM and 100mM, respectively. Finally, the proteasome inhibitor, MG132 (SML1135, Sigma), was solubilized in DMSO at 10mM concentration. All treatments were diluted to their final concentrations in media that the cells were plated in (supplemented NBM for PCNs and N2A growth media for N2A cells) before use.

2.3 Protein extraction and quantification

Following specified treatments, culture media was aspirated, cells were washed with 1×PBS and lysed with RIPA (Sigma, R0278) supplemented with 1:100 protease inhibitor cocktail (Sigma, P8340) and 1:100 phosphatase inhibitor (Sigma, P5726). The lysis

buffer was added directly to each culture dish, cells were scraped off and transferred to 1.5 mL microcentrifuge tubes and placed on ice for 30 minutes. The samples were then centrifuged at 12,000×g for 15 minutes at 4°C. The supernatant from each sample was transferred to a new labeled tube and stored in the -80°C freezer.

Protein concentration was determined by Pierce® BCA Protein Assay Kit (Thermo Scientific) according to manufacturer's protocol. Absorbance (562 nm) of samples was measured using SpectraMax® M5 Multi-Mode Microplate Reader (Molecular Devices) and SoftMaxPro V5 (Molecular Devices) software. Based on the absorbance, a standard curve was generated, and the concentration of samples were calculated based on the standards.

2.4 Glutathione assay

Reduced glutathione (GSH) was measured using monochlorobimane (MCB; Thermo Scientific, M1381MP). Primary cortical neurons were plated at 3×10^5 cells/well density in 4-well dishes. At the end of the indicated treatments, 200 µl of the media was removed from each well, leaving behind 300 µl. The MCB solubilized in DMSO (100mM) was further diluted in NBM and added to each well at a final concentration of 50 µM. The plates were incubated at 37°C for 60 minutes to allow conjugation of MCB. Cells were then washed twice with 1×PBS and were extracted for protein as described above. Once the protein was isolated, 50 µl of each sample was aliquoted to a 96-well plate and fluorescence was measured at λ_{ex} : 390 nm and λ_{em} : 478 nm in SpectraMax® M5 Multi-Mode Microplate Reader. The remainder of the protein for each sample was used to determine total protein levels for normalization purposes. GSH values were reported as relative fluorescent units (RFU)/ug of protein.

2.5 NADPH quantification

High Sensitivity NADPH Quantification Fluorometric Assay Kit (Sigma, MAK216-1KT) was used to quantify NADPH levels in each sample. To collect protein sample for each treatment condition, we pooled two 35mm dishes and lysed them in extraction buffer provided in the kit. Protein was extracted as described previously. After the supernatant

was transferred to a new microcentrifuge tube, a 50 μ l aliquot was mixed with another 30 μ l of extraction buffer and incubated at 60°C for 30 minutes to degrade NADP⁺. The samples were then incubated on ice before being aliquoted to 96-well microplate reader plate (50 μ l/sample). The NADPH standards and the reaction mix were prepared per manufacturer's instructions (Appendix A). A 100 μ l aliquot of the reaction mix was added to each well and the plate was incubated at room temperature for 60 minutes before the fluorescence was measured (λ_{ex} =535/ λ_{em} =587 nm) in the SpectraMax® M5 Multi-Mode Microplate Reader (Molecular Devices) and SoftMaxPro V5 (Molecular Devices) software. The concentration of NADPH was calculated based on the standard curve and the remainder of the protein sample was used to quantify protein concentration. NADPH levels were normalized to protein concentration for each sample.

2.6 Mitochondrial ROS detection

MitoSOX™ Red (Life Technologies, M36008) was used for staining and quantifying mitochondrial superoxide in neurons. Primary cortical neurons were plated at 3 \times 10⁵ cells/well density in 4-well dishes. At the end of the indicated treatments, 200 μ l of the media was removed from each well, leaving behind 300 μ l. MitoSOX™ Red (5mM) was diluted in NBM and was added to each well at a final concentration of 0.2 μ M. Cells were incubated at 37°C for 2 hours. Neurons were then washed twice with 1 \times PBS and fixed in 4% paraformaldehyde (containing 0.2% picric acid in 0.1M phosphate buffer, pH 7.1) for 30 minutes, then washed with 1 \times PBS again and stained with Hoechst 33342 (0.25 μ g/ml) dye. Cells were visualized under fluorescent microscope and images were captured using a CCD camera (Q-imaging, Burnaby, BC, Canada) and Northern Eclipse software (Empix imaging, Mississauga, ON, Canada). For each treatment, the total fluorescence of four different fields was measured separately and normalized to the number of the cells in each field. The average of the four fields was calculated and was considered as an “*n*” of one for each treatment.

2.7 Real time quantitative RT-PCR analysis

RNA was isolated using TRIzol® Reagent (Invitrogen) following manufacturer's protocol and the concentration was quantified on a NanoDrop1000 Spectrophotometer (Thermo Scientific). RT-PCR was performed with the Qiagen quantifast RT-PCR kit (Qiagen, 204154). All primers were purchased from Life Technologies, and the sequences are included in Appendix B. PCRs were carried out using CFX Connect™ Real Time System (BioRad, Mississauga, ON, Canada) and the RT-PCR cycling conditions were programmed as such: reverse transcription (50°C, 10 min), initial PCR activation step (95°C, 5 min), cycling step (denaturation 95°C for 10 sec; annealing and elongation 60°C for 30 sec, x 40 cycles), followed by a melting curve analysis to confirm the specificity of the primers. Changes in gene expression were determined using the $\Delta(\Delta C_t)$ method with the ribosomal S12 transcript being used for normalization. Data is reported as fold increase in mRNA levels in treated samples relative to corresponding untreated control samples for each transcript. Comparison of transcript levels at the baseline between wildtype and ATF4-deficient neurons were reported as $\Delta C_t(\text{target transcript} - \text{S12})$.

2.8 Metabolic flux assay

Oxygen consumption rate was measured using Extracellular Flux Analyzer (Seahorse Biosciences). Seahorse XFe24 tissue culture microplates (Agilent, 100777-004) were coated with poly-L-ornithine overnight and were rinsed with ddH₂O prior to plating. Primary cortical neurons were seeded at a density of 2.5×10^5 cells/ well (250µl) and were kept in the 37°C incubator for 5 days prior to assay. The day before the assay, the sensor cartridge was hydrated with calibrant media according to manufacturer's protocol (Seahorse XFe FluxPak mini, 102342-100) and was incubated at 37°C in a non-CO₂ incubator over-night. On the day of the experiment, prior to running the assay, the cells were washed with assay media: Seahorse XF base medium (Agilent, 103334-100) supplemented with 15mM glucose, 2µM L-glutamine (Gibco®, 25030-081) and 2µM sodium pyruvate (Gibco®, 11360-070), pH was adjusted to 7.4 using 0.1 N NaOH) and plates were incubated in this media in 37°C non-CO₂ incubator for 45-60 minutes.

Oxygen consumption was sequentially measured under basal conditions, in the presence of 1 μ M oligomycin, to assess ATP production, after injection of FCCP (2 μ M), to measure maximal respiration and finally in the presence of mitochondrial inhibitors, rotenone and antimycin A (1 μ M) to measure non-mitochondrial respiration. All chemicals were purchased as a kit: Seahorse XF Cell Mito Stress Test Kit (Agilent, 103015-100), and were diluted in assay media (injection ports were loaded with 80 μ l of each treatment and the starting volume in each well was 500 μ l). Immediately after the assay, cells were visualized under the microscope to ensure viability. Cells were then lysed using RIPA lysis buffer and protein was extracted as described previously for normalization purposes.

2.9 Cell death and survival assays

Live/Dead™ Viability/Cytotoxicity Kit (Molecular Probes, L3224) was used to assess cell viability. Cells plated in 4-well dishes were loaded with calcein-AM (1 μ M) and ethidium homodimer-1 (3 μ M) and incubated at 37°C for 10 minutes. Images were captured using a CCD camera (Q-imaging, Burnaby, BC, Canada) and Northern Eclipse software (Empix imaging, Mississauga, ON, Canada). Live cells were detected by the uptake of Calcein-AM (green fluorescence), while dead cells were highly permeable to ethidium homodimer-1 (red fluorescence). Four different fields were captured per well under each filter. Both live and dead cells were counted and averaged over four fields and survival was determined by the fraction of live to total cells.

2.10 Fluorescent immunocytochemistry

Primary cortical neurons were plated in 4-well dishes at a density of 3 $\times 10^5$ cells/ well and were incubated in a 37°C incubator for 5 days. Cultures were rinsed with 1 \times PBS and fixed in 4% paraformaldehyde (containing 0.2% picric acid in 0.1M phosphate buffer, pH 7.1) for 30 minutes, then washed 3 times with 1 \times PBS again before additions of cold methanol to each well for permeabilization. After 5 minutes incubation with methanol, cells were rinsed with 1 \times PBS 3 times and incubated with blocking solution (2% BSA in 1 \times TBST) for an hour at room temperature. Cultures were stained for MAP2 (Abcam, ab7513) (diluted 1:100 in blocking solution) overnight at 4°C. Cells were once again

washed with 1×PBS and incubated with Alexa Fluor™ 555 goat anti chicken (Invitrogen, A21437) (diluted 1:100 in blocking solution) for 2 hours at room temperature. Cultures were counterstained with Hoechst 33342 (10ug/mL) dye (diluted 1:1000 in 1×PBS) and were imaged using Leica-TCS sp8.

2.11 Western blot analysis

Whole cell extracts (40 µg) were separated on 12% SDS-polyacrylamide gels and transferred onto nitrocellulose membranes. Blots were probed with primary antibodies (diluted 1:1000 in blocking solution: 5% milk in TBST) against ATF4 (Abcam, ab184909) and cyclophilin (Abcam, ab178397) as loading control overnight. Membranes were then washed with TBST buffer and probed with HRP secondary (BioRad, 170-6515) diluted 1:10,000, and immunoreactive bands were visualized using Clarity™ Western ECL substrate (BioRad, 170-5061). Blots were quantified by normalizing ATF4 bands to cyclophilin.

2.12 Data analysis

Data were reported as mean and standard error of the mean (SEM). The statistical difference between groups was determined using either ANOVA and *post hoc* Tukey test or t-test. Differences were considered statistically significant with p -value<0.05. In PCNs each n value represents the number of embryos of each genotype from at least two independent neuron cultures, while in N2As each n value represents an independently prepared cell plate from a newly passaged culture.

Chapter 3

3 Results

ATF4 protein is induced in response to various stressors including ER-stress, which activates a series of signals that comprise the unfolded protein response (UPR) (Harding et al, 2000). The UPR is meant to relieve cells from stress by downregulating protein translation, enhancing protein folding by increasing the expression of specific ER chaperons, and activating proteases to degrade misfolded proteins. Prolonged ER-stress however, can lead to activation of apoptotic cell death (Liu & Kaufman, 2003). In order to upregulate endogenous ATF4, cells were treated with thapsigargin (TG). TG can cause an increase in cytosolic calcium levels since it acts as a non-competitive inhibitor of ER calcium ATPase and blocks the ability of the cell to pump calcium into the ER, which is required for ER function, and can activate the UPR (Rogers, Inesi, Wade & Lederer, 1995). We have shown previously that TG treatment induces a substantial increase in ATF4 protein levels, which can cause neuronal cell death. Consistent with this, we have shown that ATF4-deficient neurons are protected against ER-stress induced cell death (Galehdar, Swan, Fuerth, Callaghan, Park & Cregan, 2010). Therefore, in this study, we used TG-induced ER stress as a model of ATF4-dependent cell death.

3.1 Primary cortical cultures from both wildtype and ATF4-deficient mice are mainly neuronal

Firstly, to confirm that our primary cortical cultures were healthy and were mainly neuronal, cultures were stained with microtubule-associate protein (MAP2) as a neuronal marker at 5 days *in vitro* (DIV). Nuclei were also identified using Hoechst stain. Immunostaining results showed that in both WT and ATF4-deficient cultures, more than 90% of the cells were stained with MAP2 suggesting that both cultures are primarily neuronal (Figure 3.1).

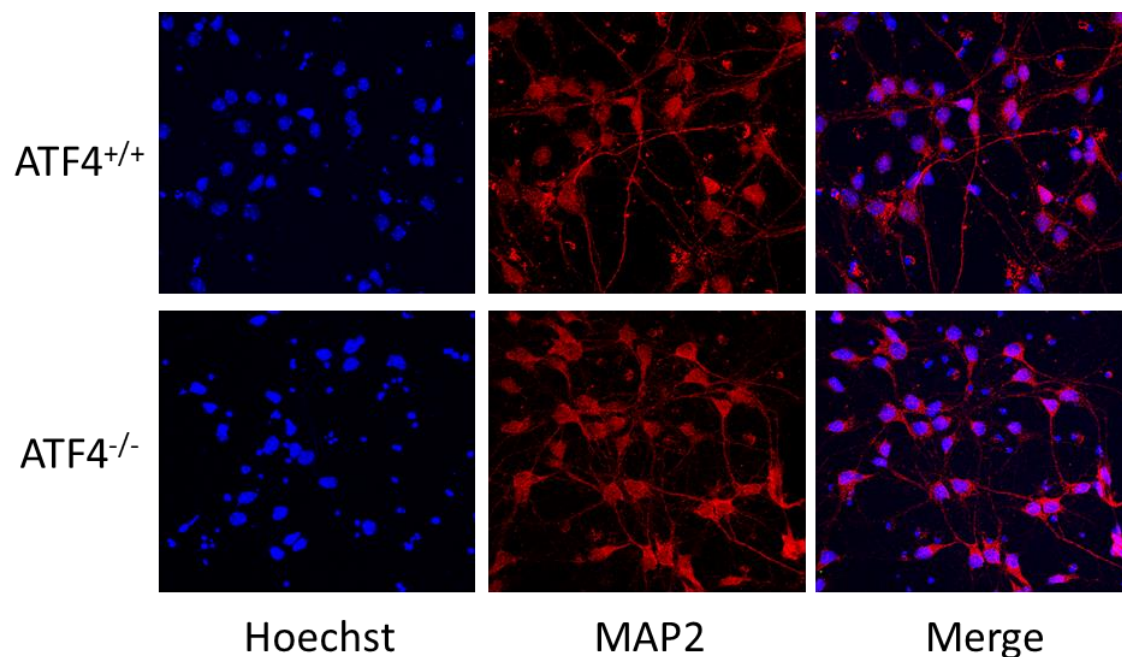


Figure 3.1. Primary cortical cultures are mainly neuronal. WT and $ATF4$ -deficient cortical cultures were stained with MAP2 at 5 DIV and images were taken using Leica TCS sp8. Fluorescent images showed that both $ATF4^{+/+}$ and $ATF4^{-/-}$ cultures are healthy and are primarily neuronal. Images were taken at 40x magnification.

3.2 Wildtype neurons retain GSH more efficiently compared to ATF4-KO cells in the presence of ER-stress

A previous study suggested that ectopic overexpression of ATF4 depletes GSH levels in cortical neurons (Lange et al, 2008), therefore we examined endogenously upregulated ATF4 effects on GSH levels. To address this, we extracted primary cortical neurons from wildtype and ATF4-deficient mice and allowed them to mature in culture for 5 days after plating. Neurons were treated with TG for 12 or 24 hours to induce ATF4 protein levels and GSH was measured using a Monochlorobimane (MCB) assay. Our results showed no difference in GSH levels between WT ($n=15$) and ATF4-deficient ($n=15$) neurons in untreated cultures. Furthermore, although TG treatment caused a reduction in GSH levels in both WT (12_hours: ns, 24_hours: $##p<0.01$) and ATF4-deficient neurons (12_hours: $#p<0.01$, 24_hours: $####p<0.0001$), the reduction was significantly greater in the absence of ATF4 at both 12 hours (WT: $n=12$, ATF4-KO: $n=12$) ($***p<0.001$) and 24 hours (WT: $n=12$, ATF4-KO: $n=12$) ($**p<0.01$) post-treatment (Figure 3.2). This suggests that endogenous ATF4 upregulation acts to sustain GSH levels during ER-stress.

3.3 ATF4^{+/+} neurons consume GSH more rapidly compared to ATF4-deficient cells in the presence of ER-stress

The steady state level of GSH in cells reflects relative levels of its *de novo* synthesis, utilization and regeneration. To narrow down the part of the pathway that is affected by ATF4, *de novo* synthesis of GSH was blocked using L-buthionine sulfoximine (BSO). BSO blocks the rate limiting step in GSH synthesis by inhibiting the enzyme glutamylcysteine ligase (GCL) (Drew & Minors, 1984). Therefore, GSH levels measured in the presence of BSO reflect reserved GSH and GSH regenerated by the reduction of oxidized GSH. Neurons were co-treated with TG to induce endogenous ATF4 protein expression. Interestingly, when GSH synthesis was inhibited, an opposite trend of GSH loss was observed compared to TG treated neurons alone (Figure 3.2), where after 24h of TG and BSO co-treatment, WT ($n=9$) cells exhibited lower levels of GSH compared to ATF4-KO ($n=9$) neurons ($*p<0.05$) (Figure 3.3a). This suggests that ATF4 promotes

GSH synthesis in stressed neurons, however, it would appear that ATF4 also induces a more rapid consumption of GSH compared to ATF4-deficient cells in the presence of ER-stress. To confirm that the observed results were the combined effect of TG and BSO and not BSO alone, the experiment was repeated in the presence of BSO only. Our results showed that under non-stressed conditions, after 12 (WT: $n=4$, KO: $n=5$) and 24 (WT: $n=9$, KO: $n=8$) hours of BSO treatment, both WT and ATF4-KO neurons had the same level of GSH, highlighting the fact that the difference that was observed during ER-stress, was due to the combined effect of TG-induced ATF4 induction and BSO (Figure 3.3b). Next, we investigated two possible mechanisms to explain why WT neurons lose GSH more rapidly compared to ATF4-deficient neurons.

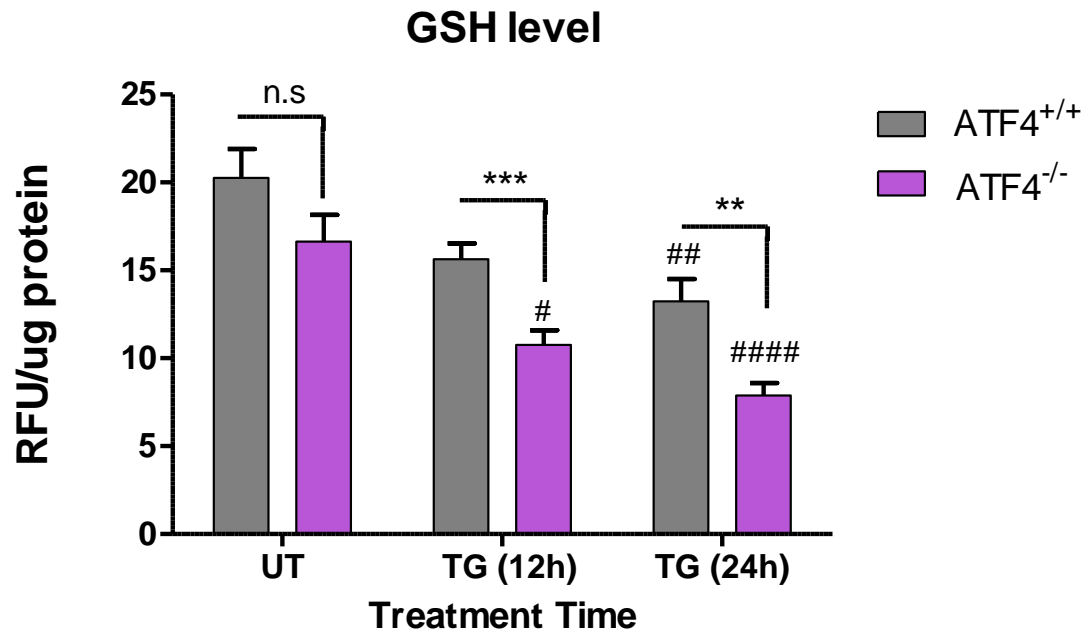


Figure 3.2. $\text{ATF4}^{+/+}$ neurons retain GSH levels to a greater extent compared to $\text{ATF4}^{-/-}$ neurons after induction of prolonged ER-stress. Cortical neurons were extracted from E14.5-15.5 $\text{ATF4}^{+/+}$ and $\text{ATF4}^{-/-}$ littermates. Cultures were treated with TG (1- μM) and GSH levels were measured at 12 and 24 hours by MCB assay. ER-stress reduced GSH levels in both WT (24_h: $##p < 0.01$) and $\text{ATF4}^{-/-}$ (12_h: $\#p < 0.01$, 24_h: $####p < 0.001$) neurons, but the reduction was more significant in ATF4 -deficient cells at both 12 ($***p < 0.001$) and 24 ($**p < 0.01$) hours. # signifies comparison to the untreated (UT) control. n values: UT WT/KO ($n=15$); 12 & 24_h TG WT/KO ($n=12$).

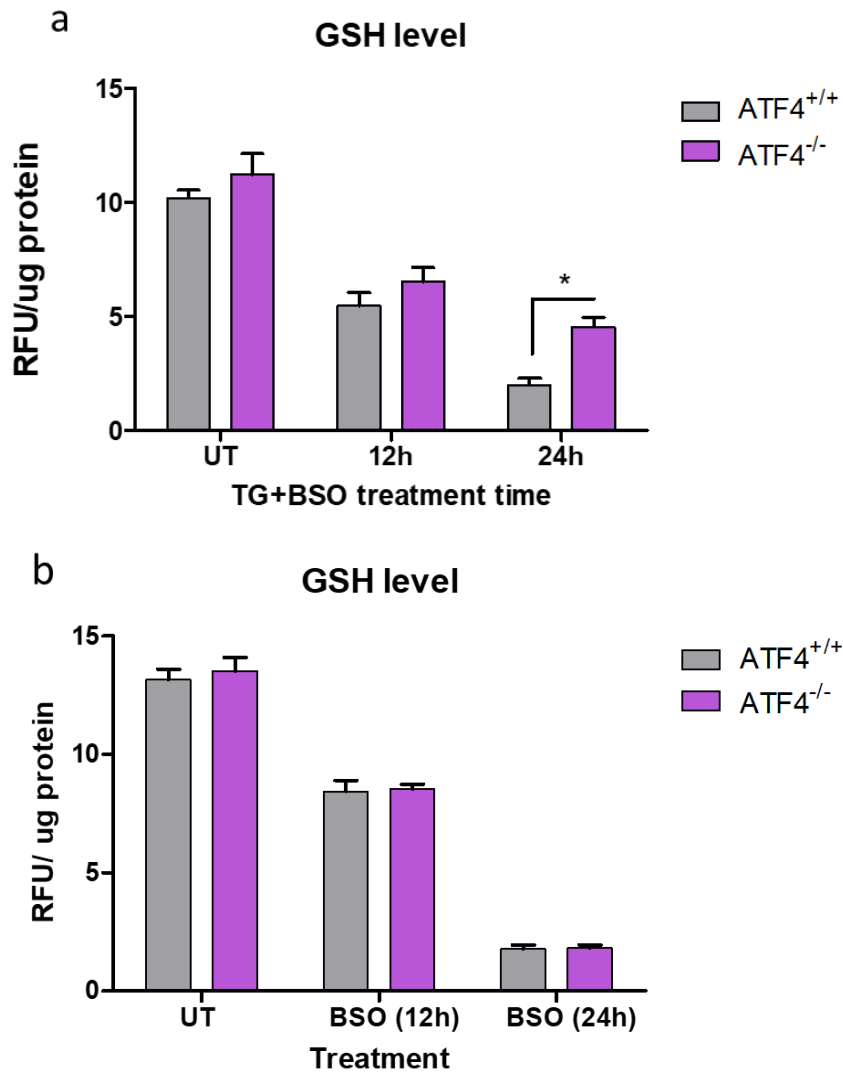


Figure 3.3. Endogenous upregulation of ATF4 increases GSH consumption. Cortical neurons were extracted from E14.5-15.5 ATF4^{+/+} and ATF4^{-/-} littermates. (a) cultures were co-treated with 100- μ M BSO and 1- μ M TG. GSH was measured 12 and 24 hours post treatment. After 24h of co-treatment with TG and BSO, ATF4-deficient neurons ($n=9$) had higher levels of GSH compared to the WT ($n=9$) cells ($*p<0.05$) (b) when cells were treated with BSO (100- μ M) only, there was no difference between GSH levels at either of the timepoints. n values: UT WT/KO ($n=13$); 12h BSO WT ($n=4$), KO ($n=5$); 24h BSO WT ($n=9$), KO ($n=8$).

3.4 GSH regeneration pathway is not affected by ATF4 in neurons

We next examined whether the higher GSH reserve in ATF4-deficient neurons was related to a potential difference in GSH regeneration capacity. The two important factors that are required for GSH regeneration are glutathione reductase (GR), which is the enzyme responsible for reducing GSH from its oxidized form (GSSG), and NADPH, which is the essential reducing agent in this process. In order to assess GSH regeneration capacity, we measured both GR transcript level as well as NADPH levels. To measure GR mRNA levels, cortical neurons were treated with TG and RNA was collected after 8 hours and relative mRNA levels were determined by qRT-PCR. Our results show that ER-stress causes a downregulation in GR transcription compared to the control (WT: *** $p < 0.001$; KO: *** $p < 0.001$), although this occurs in an ATF4-independent manner (Figure 3.4a). Furthermore, comparison of mRNA levels at the baseline between WT and ATF4-deficient cells showed no difference between the two genotypes (Figure 3.4b). We also measured NADPH levels at baseline and after treatment with TG. Results showed that although ER-stress caused a reduction in NADPH levels in both WT ($n=4$) and ATF4-KO ($n=3$) neurons compared to untreated controls, the percent reduction compared to baseline was not significantly different between the two genotypes (Figure 3.4c). Taken together, these results suggest that GSH regeneration capacity is not affected by ATF4 in cortical neurons.

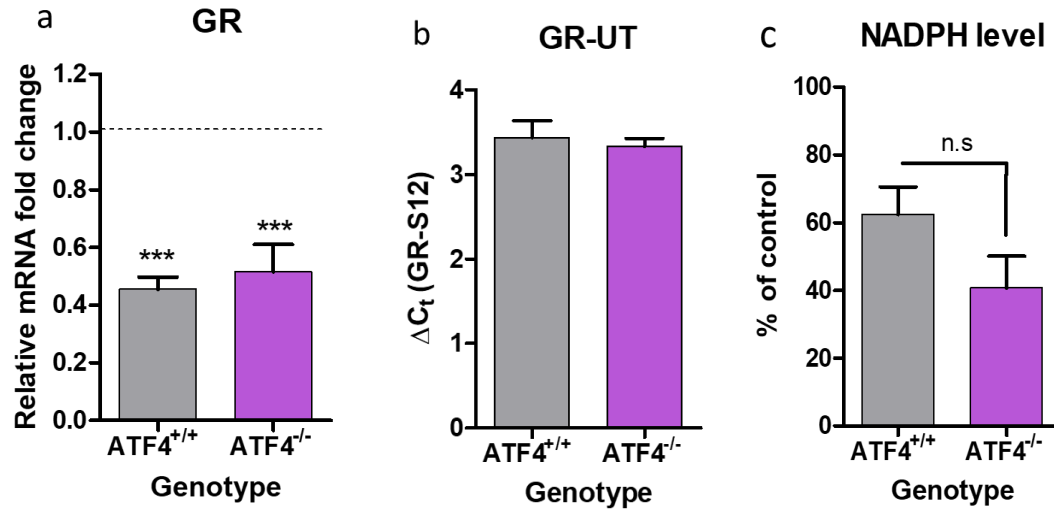


Figure 3.4. GSH regeneration pathway is not affected by ATF4. PCN were extracted from E14.5-15.5 ATF4^{+/+} and ATF4^{-/-} littermates. (a,b) Neurons (5 DIV) were treated with 1- μ M TG for 8 hours and mRNA levels of GR was determined by qRT-PCR. TG treatment reduced GR mRNA levels compared to the control in both WT (*** p <0.001) and ATF4-deficient (*** p <0.001) neurons (n =4), although the reduction was independent of ATF4 (b) GR mRNA levels are not significantly different in untreated WT and ATF4-deficient neurons (n =4). (c) Neurons were treated with 1- μ M TG for 9 hours and NADPH levels were determined by quantitative fluorometric assay. TG treatment reduced NADPH levels compared to control in both WT (n =4) and ATF4-deficient (n =3) neurons in an ATF4-independent manner.

3.5 ATF4 does not affect mitochondrial ROS production

In an effort to explain why WT neurons consume GSH more rapidly compared to ATF4-deficient cells, we next investigated whether the level of oxidative processes differs between WT and ATF4-deficient neurons. To evaluate this, we quantified mitochondrial superoxide as a measure of ROS production in ATF4^{+/+} and ATF4^{-/-} neurons.

3.5.1 ER-stress affects mitochondrial bioenergetics in an ATF4-independent manner

In order to ensure that our treatment paradigm affects different aspects of mitochondrial respiration and that mitochondrial superoxide would be a reliable measure for ROS, we analyzed different aspects of mitochondrial respiration by measuring the oxygen consumption rate (OCR) of the cells under various conditions using Seahorse Mito Stress test. Results showed that TG treatment caused a reduction in basal respiration as well as ATP production, while it did not influence maximal respiration or spare respiratory capacity (Figure 3.5). However, the effect of TG on mitochondrial bioenergetics was not ATF4-dependent. These results imply that mitochondrial superoxide can serve as an appropriate measure of ROS level since our ER-stress paradigm has significant effects on mitochondrial bioenergetics.

3.5.2 ER-stress induces mitochondrial superoxide production is independent of ATF4 upregulation

To determine whether ATF4 expression affects mitochondrial superoxide production, WT and ATF4-deficient neurons were treated with TG and BSO, and superoxide production was assessed by MitoSOX™ Red. TG treatment increased the level of mitochondrial superoxide production, however, the superoxide levels did not differ between ATF4^{+/+} and ATF4^{-/-} neurons (Figure 3.6). This suggests that ATF4 expression does not affect ER-stress induced oxidative processes. Furthermore, depletion of GSH using BSO in the absence of any stressors did not have an effect on mitochondrial superoxide levels.

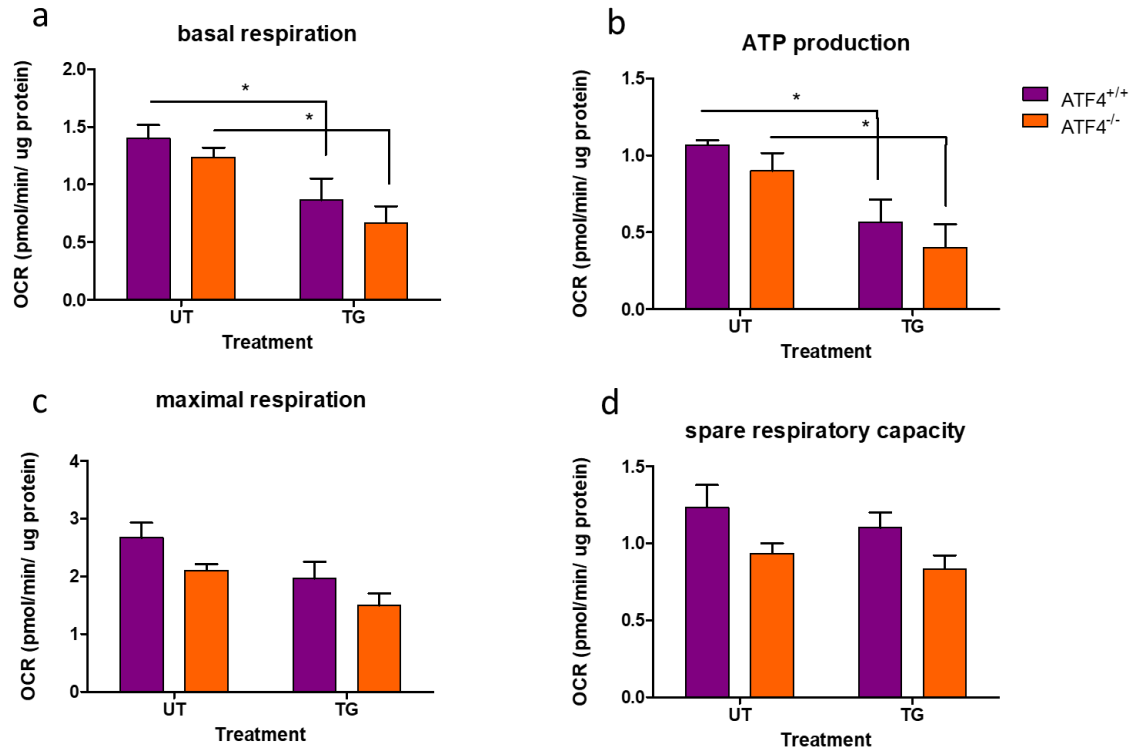


Figure 3.5. TG treatment affects mitochondrial bioenergetics in an ATF4-independent manner. PCN were extracted from E14.5-15.5 ATF4^{+/+} and ATF4^{-/-} littermates and were plated in Seahorse XFe24 tissue culture microplates at a density of 2.5×10^5 cells/well. Cells were incubated at 37°C with 5% CO₂ for 5 days prior to performing the assay. Cultures were treated with 1-μM TG for 12 hours and the Seahorse Mitostress test was performed to assess key parameters of mitochondrial function by directly measuring the OCR in each culture. The assay revealed that TG treatment has an impact on (a) basal respiration *p-value<0.05 and (b) ATP production *p-value<0.05 in both WT (n=3) and ATF4-deficient (n=3) neurons. (c) maximal respiration and consequently the (d) spare respiratory capacity are not significantly affected by the treatment.

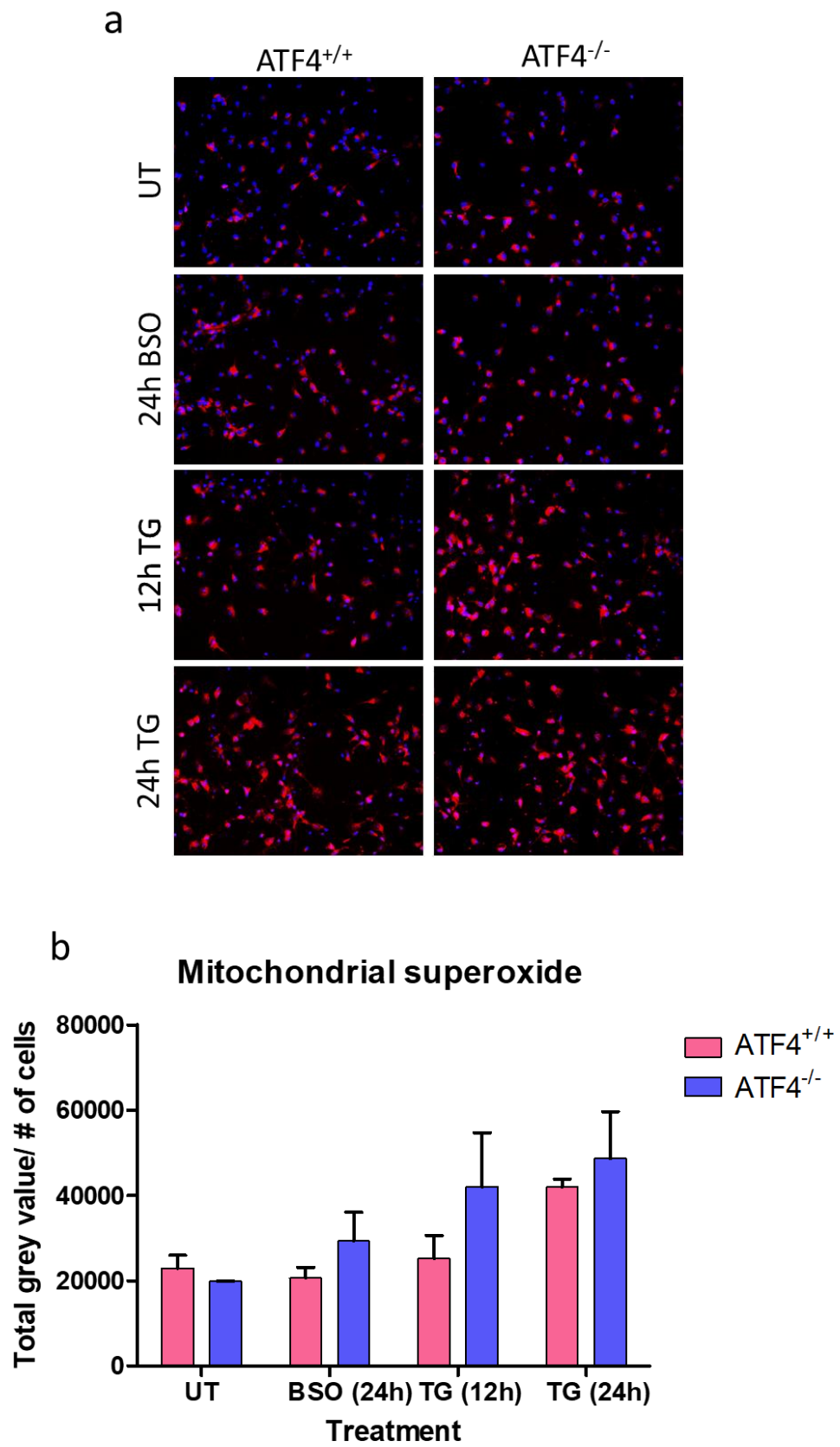


Figure 3.6. Mitochondrial superoxide production is independent of ATF4 upregulation. PCN were extracted from E14.5-15.5 ATF4^{+/+} and ATF4^{-/-} littermates (*a*) and neurons were treated with BSO (100- μ M) for 24 hours or with TG (1- μ M) for 12 and 24 hours. Cultures were then loaded with 0.2- μ M MitoSOX Red for 2 hours to detect mitochondrial derived superoxide. Cells were also counter-stained with Hoechst 33342 and the fluorescence of each field was normalized to the number of the cells in that field (*b*) quantification of MitoSOX Red fluorescence after normalization showed no difference between the two genotypes under any of the treatment conditions.

3.6 Endogenous ATF4 upregulation affects the gene expression profile of GSH related factors

Since neither GSH regeneration capacity nor the extent of oxidative processes could account for why ATF4-deficient neurons are more efficient at maintaining GSH levels, or why WT cells lose GSH more rapidly when the *de novo* synthesis of GSH is blocked, we investigated various gene transcripts that are important for GSH degradation and synthesis. *ChaC1* encodes glutathione-specific gamma-glutamylcyclotransferase 1, which is important for degradation of GSH. To measure transcript levels of this gene, cells were treated with TG for 8 hours and total RNA was isolated for performing qRT-PCR. Analysis of qRT-PCR results showed that *ChaC1* is induced in WT ($n=3$) cells treated with TG but not ATF4-KO ($n=3$) neurons ($*p<0.05$) (Figure 3.7a). This finding suggests that WT neurons may degrade GSH more rapidly compared to the ATF4-KO, which might partly explain why the WT cells have lower levels of GSH compared to the ATF4-deficient neurons after induction of prolonged ER-stress (Figure 3.3a).

For GSH synthesis, we assessed the expression of two different transcripts: *GCL*, which catalyzes the rate limiting step in synthesis of GSH and *SLC7A11*, which encodes a cystine-glutamate antiporter, also known as system x_c^- , which is important for the uptake of precursors for synthesis of GSH. Cultures were treated with TG for 8 hours, total RNA was isolated from the samples and transcript levels were measured using qRT-PCR. Results showed no difference in *GCL* mRNA level between WT ($n=4$) and ATF4-KO ($n=4$) neurons (Figure 3.7b). In fact, ER-stress did not have any effect on *GCL* transcript levels in neurons from either genotype. Interestingly, evaluation of *SLC7A11* mRNA level showed an ATF4-dependent increase in neurons after treatment with TG ($**p<0.01$) (Figure 3.7c). This finding may suggest that even though WT cells might degrade GSH more rapidly, they compensate for it by increasing the rate of GSH synthesis. It also explains why the WT cells lose GSH more rapidly once *de novo* synthesis of GSH is inhibited.

The mRNA level for each gene was also measured at baseline relative to S12 control in both WT and ATF4-deficient cells and was reported as ΔC_t . Results suggested that ATF4

did not have an effect on basal mRNA levels of any of these glutathione related transcripts (Figure 3.7d, e, f).

3.7 Replenishment of the antioxidant pool does not protect neurons against ER-stress-induced cell death

In the previous report by Lange et al. (2008) it was shown that the cell death that result from ectopic overexpression of ATF4 can be ameliorated by treating cells with an antioxidant such as butylated hydroxyanisole (BHA). Therefore, we examined whether addition of antioxidants might be protective in an endogenous ATF4-dependent cell death paradigm. We performed a live/dead assay on neurons treated with TG ($n=11$), TG in combination with N-acetylcysteine (NAC) ($n=11$), which is an antioxidant and acts as a precursor for GSH synthesis, as well as TG in combination with BHA ($n=9$), which is another well-characterized antioxidant, for 30 hours. As shown in figure 3.8 (a, b), TG treatment reduced cell viability as expected (** $p < 0.01$). However, contrary to what was reported by Lange et al, following ectopic expression of ATF4, addition of antioxidants did not have a significant effect on cell viability in endogenous ATF4-dependent neuronal death (Figure 3.8a, b). Furthermore, the effect of each antioxidant alone was also examined on cell viability and it was confirmed that the concentrations used were not toxic to the cells (Figure 3.8 c, d).

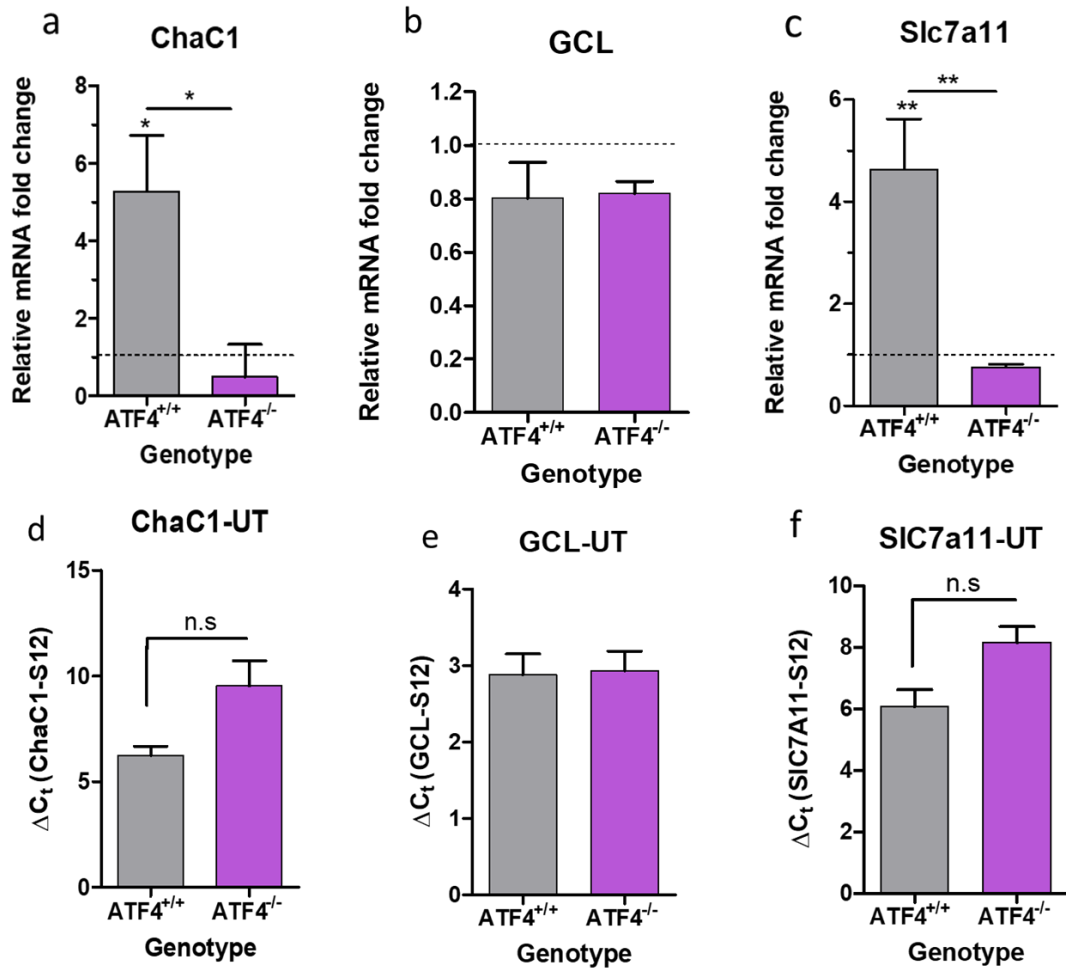


Figure 3.7. ATF4 upregulation causes differential transcription of GSH-related genes. PCNs extracted from E14.5-15.5 ATF4^{+/+} and ATF4^{-/-} littermates were treated with 1- μ M TG for 8 hours and RNA was isolated using TRIzol® Reagent and the expression of glutathione related transcripts was assessed by qRT-PCR. Relative mRNA levels are reported as fold increase in TG treated neurons as compared to untreated neurons. (a) ChaC1 was induced in response to ER-stress in WT ($n=3$) neurons but not in ATF4-KO ($n=3$) cells (* $p<0.05$) (b) GCL mRNA level was not affected by ER-stress in WT ($n=4$) or ATF4-deficient ($n=4$) cells (c) SLC7A11 transcript was induced in WT ($n=3$) cells treated with TG but not in ATF4-deficient ($n=3$) neurons (** $p<0.01$). The * on each bar represents significance compared to untreated control (d,e,f) relative expression of each transcript was measured at the baseline in both WT and ATF4-deficient neurons and was reported as ΔC_t (C_t (GOI)- C_t (S12)). Results indicate that the mRNA levels of ChaC1, GCL, or SLC7A11 in untreated ATF4^{+/+} and ATF4^{-/-} neurons is not significantly different.

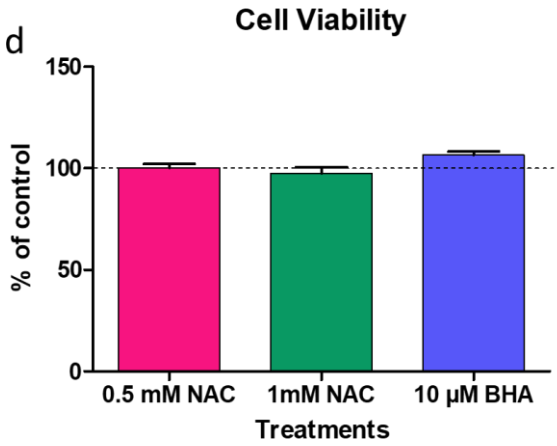
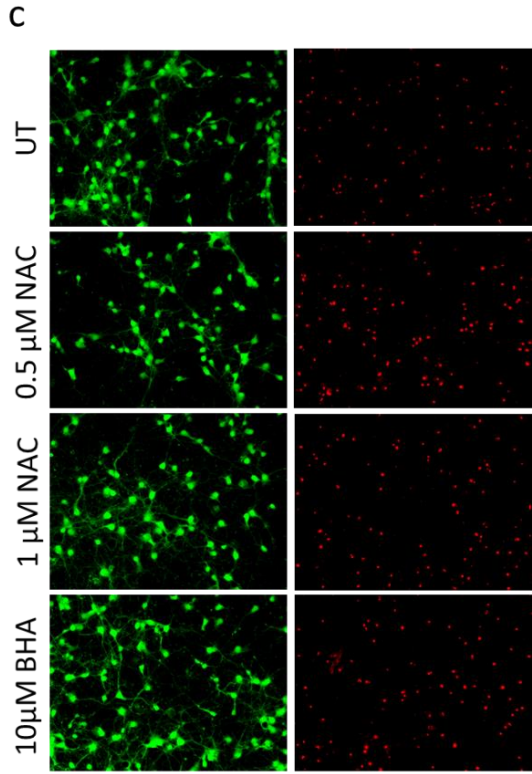
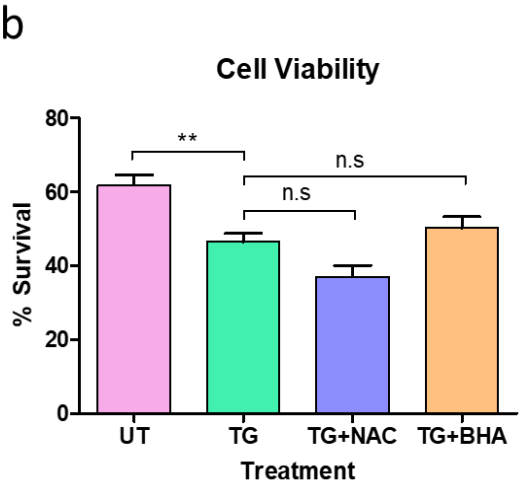
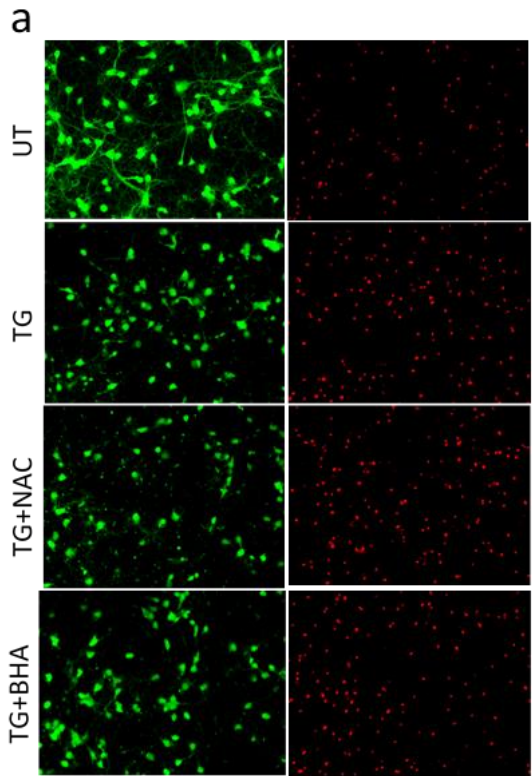


Figure 3.8. Replenishment of the antioxidant pool does not protect neurons against cell death. PCN were extracted from E14.5-15.5 C57/BL6 embryos and were cultured at a density of 3×10^5 cells/well. Cells were treated as specified for 30 hours and were loaded with calcein-AM (1- μ M) and ethidium homodimer-1 (3- μ M) for 10 minutes. (a) Representative live/dead assay images showing untreated, TG treatment (1- μ M) ($n=11$), TG (1- μ M)+NAC (1-mM) ($n=11$) and TG (1- μ M)+BHA (10- μ M) ($n=9$). (b) quantification of all trials ($n=11$ for UT, TG, TG+NAC, $n=9$ for NAC+BHA). In any single trial, 4 different fields in each well were imaged under each filter. All four fields were counted and averaged to yield an $n=1$ ** p -value<0.001 (c, d) treatment with BHA and NAC alone did not affect cell viability compared to control ($n=3$).

3.8 ATF4 protein levels can be upregulated/stabilized in the presence or absence of ISR

The aim of this project was to investigate whether upregulation of endogenous ATF4 is sufficient to reduce GSH levels in neurons, and to identify key players in this process. Our findings demonstrate that unlike ectopically overexpressed ATF4, upregulation of endogenous ATF4 does not reduce GSH levels. To further investigate this differential observation, transcriptional activity of ATF4 was assessed after the protein was stabilized by different mechanisms in both N2As and primary cortical neurons (PCNs). Three different mechanisms were used to stabilize ATF4 protein in N2A cells, which included activation of ISR using TG treatment that allows for expression of ATF4 through post-transcriptional modifications, inhibition of proteasome using MG132 treatment, which prevents degradation of ATF4 protein and stabilizes it post-translationally, and finally ectopic overexpression of the protein through plasmid transfection. In PCNs, a method to ectopically overexpress the protein was not available, but ATF4 was still stabilized using TG and MG132 treatments. Western blot analysis showed that all three mechanisms led to a significant increase in ATF4 protein levels, suggesting that the chosen mechanisms are effective in stabilizing ATF4 protein (Figure 3.9).

3.9 Downstream target genes that are induced by ATF4 differ, depending on how ATF4 is expressed or stabilized.

After confirming that ATF4 protein is upregulated in response to different treatments, we performed a qRT-PCR to assess the expression of different downstream targets of ATF4 including some known pro-apoptotic targets such as CHOP and Trib3, as well as other ones whose roles are still not fully understood such as ATF3 and 4E-BP1. Our results showed that when ATF4 was activated through the conventional ISR pathway, the ATF4-regulated pro-apoptotic target genes, CHOP and Trib3 were more robustly induced compared to ectopically overexpressed ATF4 and post-translationally stabilized endogenous ATF4 in both N2As and PCNs (Figure 3.10). In contrast, ATF4 stabilized post-translationally using MG132 treatment induced the expression of ATF3 more

robustly than ISR-induced and ectopically overexpressed ATF4 in both N2A cells and PCNs (Figure 3.10). There are also other target genes such as 4E-BP1 that is induced in PCNs but not N2A cells (Figure 3.10). This further highlights a cell type dependent activity of ATF4 since some target genes are only induced in one cell-type but not another. Interestingly, we found that despite the high level of ATF4 expression observed in N2A cells transfected with pc-DNA3-mATF4 (Figure 3.9b), there was not a significant induction of any of these ATF4 target genes (Figure 3.10a). These results suggest that the downstream gene targets of ATF4 differ depending on the cells type and the context of ATF4 expression, which might partly explain the differential results observed in terms of its effect on GSH levels.

Since we observed differences in the induction of known ATF4 target genes based on the context of ATF4 expression, we therefore assessed whether these differences persist in GSH related transcripts. We previously showed that ChaC1 and SIC7A11 are induced in WT neurons, when ATF4 is expressed through ISR activation (Figure 3.7a,c). We then measured the level of mRNA induction of these genes in N2A cells after stabilization of ATF4 post-transcriptionally through ISR, post translationally through proteasome inhibition, and also through ectopic overexpression using pcDNA3-mATF4. Our results showed that ISR-induced ATF4 ($n=4$) increases the expression of ChaC1 and SIC7A11 mRNA more robustly than post-translationally stabilized ATF4 ($n=5$) (ChaC1: $*p<0.05$; SIC7A11: $**p<0.01$) (Figure 3.11). Furthermore, consistent with our previous data, ectopically overexpressed ATF4 ($n=4$), did not induce either of the GSH-related target genes (Figure 3.11). These data further highlight the importance of the context of ATF4 expression in the induction of its downstream target genes and further confirm that the disparity between our observations in terms of GSH is due to the differential mode of ATF4 activation.

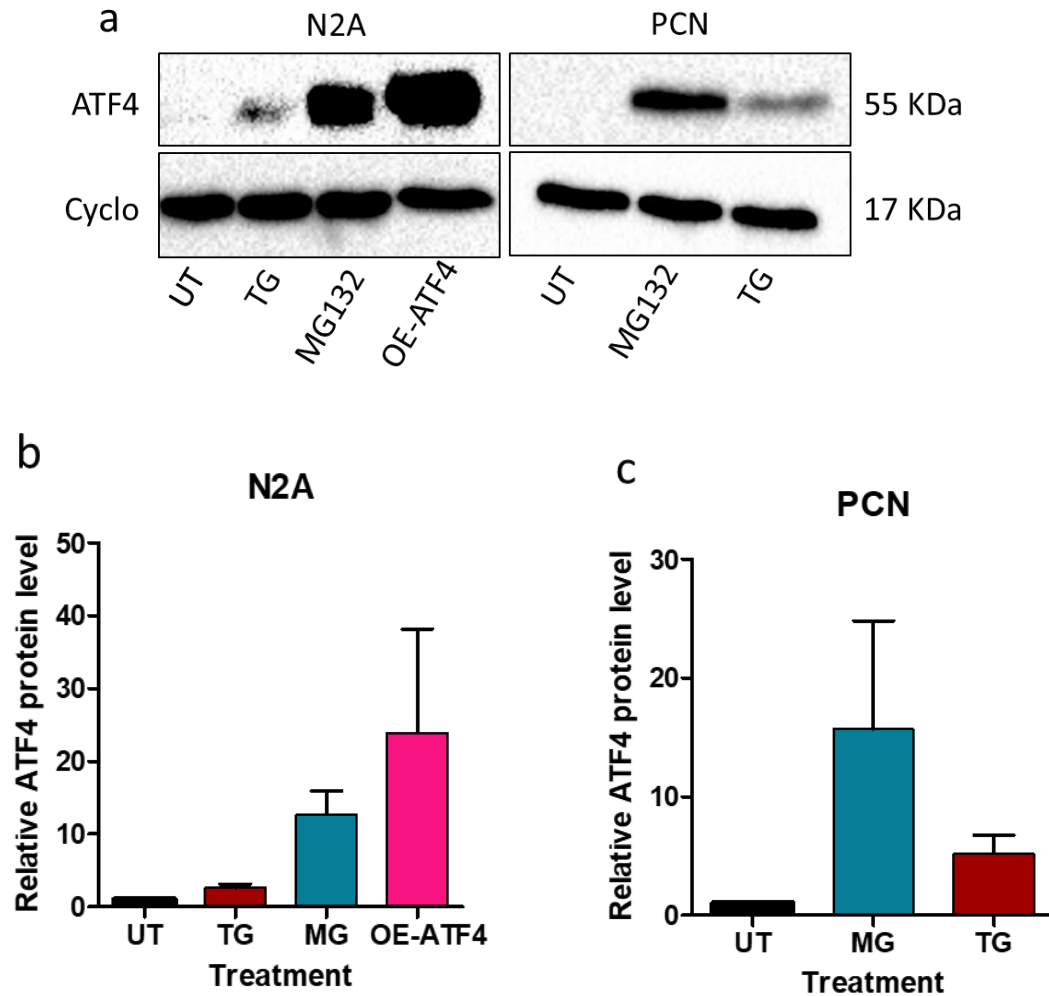


Figure 3.9. ATF4 protein levels are increased in response to various treatments. N2As and PCNs were treated with 1- μ M TG or 10- μ M MG132 for 8 hours. N2A cells were also transfected with pcDNA3-mATF4. Protein was extracted and immunoblotted for ATF4 and cyclophilin-B as a loading control. (a) Representative blots showing ATF4 protein expression under described conditions in both N2A and PCNs (b) quantification of ATF4 upregulation in response to TG and MG132 treatments, and after plasmid overexpression in N2A cells ($n=4$) (c) quantification of ATF4 protein level following treatment with MG132 and TG in PCNs ($n=5$).

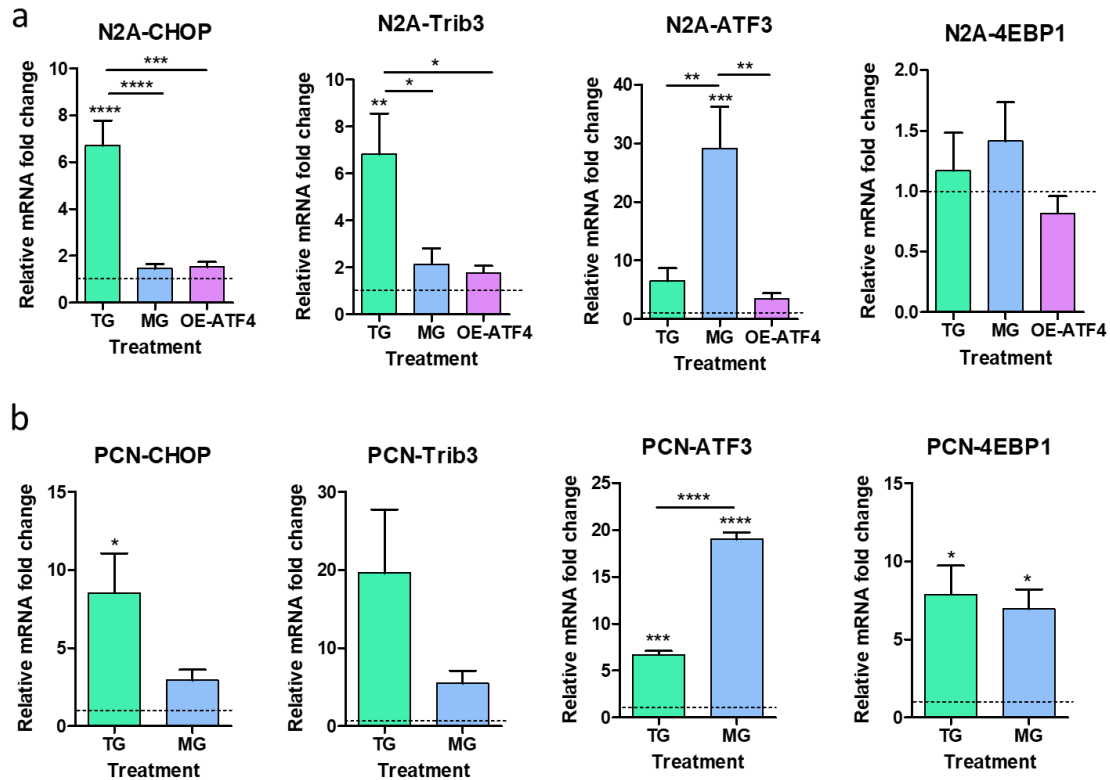


Figure 3.10. Downstream target genes that are induced by ATF4 differ, depending on the cell type and mechanism of ATF4 expression. N2As and PCNs were treated with 1- μ M TG or 10- μ M MG132 for 8 hours. N2A cells were also transfected with plasmid DNA expressing ATF4 (pcDNA3-mATF4). Total RNA was isolated and relative mRNA levels of the indicated transcripts was determined by qRT-PCR. (a) In N2A cells, TG treatment ($n=5$) induced CHOP and Trib3 to a greater extent as compared to MG132 ($n=5$) ($****p<0.0001$, $*p<0.05$), and OE-ATF4 ($n=4$) ($***p<0.001$, $*p<0.05$), while the induction of ATF3 was more significant with MG132 compared to TG treatment ($**p<0.01$) and OE-ATF4 ($**p<0.01$). 4E-BP1 induction was not significant under any of the treatment conditions. (b) The trend of mRNA induction of the target genes in the cortical neurons also followed what was observed in N2As, with TG ($n=3$) inducing CHOP ($*p<0.05$) and Trib3, and MG132 ($n=3$) inducing ATF3 ($****p<0.0001$) more robustly.

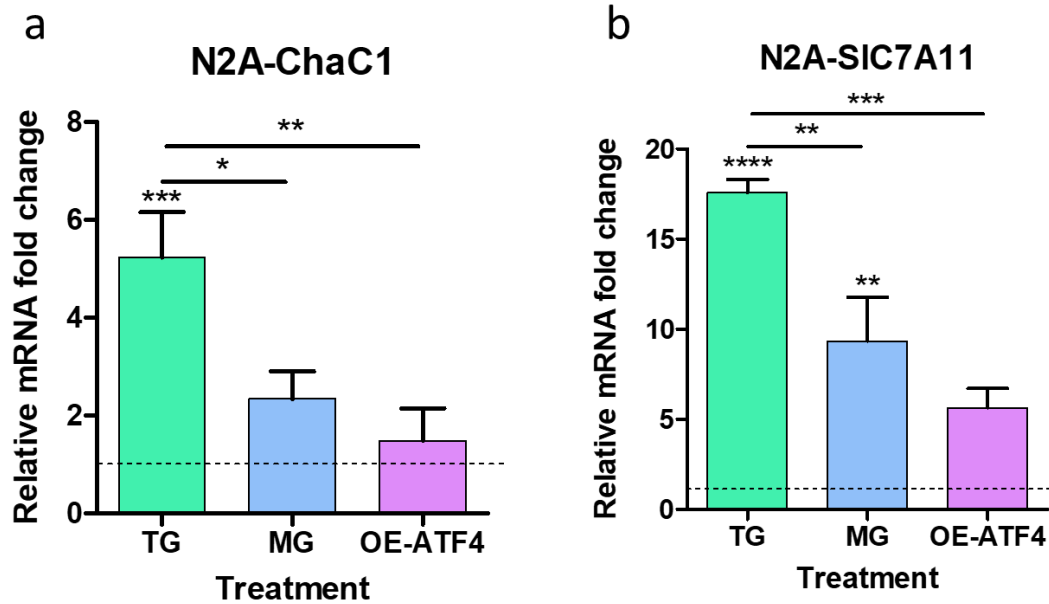


Figure 3.11. The mechanism of ATF4 expression affects the induction of GSH related transcripts. N2A cells were treated with 1- μ M TG or 10- μ M MG132 for 8 hours. Cells were also transfected with plasmid DNA expressing ATF4 (pcDNA3-mATF4). Total RNA was isolated and relative mRNA levels of the indicated transcripts was determined by qRT-PCR. (a) TG treatment ($n=4$) induced ChaC1 significantly more compared to MG132 treatment ($n=5$) ($*p<0.05$) and overexpressed ATF4 ($n=4$) ($**p<0.01$). (b) TG treatment ($n=4$) also induced a more robust expression of SIC7A11 compared to MG132 treatment ($n=5$) ($**p<0.01$) as well as overexpressed ATF4 ($n=4$) ($***p<0.001$). * above each bar indicates significance compared to control.

Chapter 4

4 Discussion

4.1 ATF4 plays a role in GSH synthesis

ATF4 is a bZIP transcription factor that is induced in response to various cell stressors such as oxidative and ER-stress as part of the integrated stress response (ISR). Although initially, induction of ATF4 acts to alleviate stress, prolonged activation of ATF4 has been shown to be pro-apoptotic in neurons and other cell types (Harding et al, 2003, Lange et al, 2008; Galehdar et al, 2010). ATF4 can promote cell death through the transcriptional induction of pro-apoptotic factors such as CHOP and Trib3 (Galehdar et al, Aimé et al, 2015). However, there is also evidence suggesting that ectopic overexpression of ATF4 in primary cortical neurons can lead to depletion of cellular GSH levels, which is an important antioxidant (Lange et al, 2008). Interestingly, the same report suggested that cell death caused by overexpression of ATF4 could be ameliorated by the addition of antioxidants, suggesting that the observed cell death is a consequence of GSH depletion (Lange et al, 2008). Consistent with this, we have previously demonstrated that depletion of GSH can sensitize neurons to oxidative stress-induced cell death (Baxter et al, 2015). In this project, an ATF4-dependent cell death paradigm was used to examine whether GSH depletion and oxidative stress are also consequents of endogenously upregulated ATF4. To address this, WT and ATF4-deficient neurons were treated with thapsigargin (TG), which is an ER-stressor and an activator of the integrated stress response (ISR) that we have previously shown to induce neuronal cell death in an ATF4-dependent manner. After a prolonged period of ER-stress, glutathione (GSH) levels were measured in these cells. The results showed that unlike ectopically overexpressed ATF4, endogenous upregulation of ATF4 through activation of the ISR enabled WT cells to maintain higher levels of GSH than ATF4-deficient neurons (Figure 3.2). Intracellular GSH levels are regulated through three main mechanisms: synthesis, utilization and regeneration. To determine which part of the GSH pathway was affected

by ATF4 expression, neurons were treated with TG, while *de novo* synthesis of GSH was blocked using BSO, which inhibits glutamylcysteine ligase (GCL), an enzyme that catalyzes the rate limiting step in GSH synthesis. Therefore, inhibition of GSH synthesis using BSO, allows for indirect measurement of the other two mechanisms, regeneration and utilization. This way, we control for possible differential rates of synthesis and only measure the GSH reserve as well as regenerated GSH in the cultures. Interestingly, our results showed that when GSH synthesis is inhibited under stress conditions, WT neurons lost GSH more rapidly than ATF4-deficient neurons (Figure 3.3a); an opposite trend to what was observed in the absence of the GCL inhibitor. Taken together, these results suggest that endogenous ATF4 upregulation leads to a more rapid loss of GSH in neurons but compensates for this by increasing the rate of GSH synthesis.

As mentioned earlier, indirect measurement of regenerated and reserved GSH indicated that WT cells have lower levels compared to ATF4-deficient neurons (Figure 3.3a). To further narrow down the part of the pathway affected by ATF4, we first assessed whether the obtained results were due to a differential rate of GSH regeneration by measuring the levels of various key players in the pathway including glutathione reductase (GR) activity and gene transcript levels as well as NADPH concentrations. GR is the enzyme responsible for regeneration of reduced GSH from its oxidized form, GSSG, and it uses NADPH as a precursor in this process (Maher, 2005). GSH regeneration is important since decreased GSH: GSSG ratio has been associated with oxidative stress and has been seen in post mortem brain of patients with AD and PD (Ballatori, Krance, Notenboom, Shi, Tieu & Hammond, 2009; Ansari & Scheff, 2010; Dexter et al, 1994; Sian et al, 1994). Initially, we attempted to directly measure GR activity as well as GSH: GSSG ratio, however, due to high variability and low sensitivity of the assays, our efforts were mainly unsuccessful. Therefore, instead of direct measurement of GR activity, we measured GR transcript levels as a correlate of its activity, even though this poses limitations for interpretation of the data. Our qRT-PCR results showed that ER-stress caused a reduction in GR mRNA but that this was not dependent on ATF4 (Figure 3.4a). The fact that GR transcript levels are decreased under ER-stress condition is surprising considering that under these conditions, oxidative processes in the cells are increased (Figure 3.6) and the cells utilize GSH more rapidly (Figure 3.2) and hence require an

efficient regeneration capacity in order to maintain physiologic GSH: GSSG ratio. Measurement of NADPH levels, in ATF4^{+/+} and ATF4^{-/-} cortical neuron cultures also showed that ER-stress decreased NADPH in an ATF4-independent manner (Figure 3.4c). The main source of intracellular NADPH is the pentose phosphate pathway (PPP) (Maher, 2005). It has been shown that shunting of the glucose away from the PPP in neurons leads to rapid neuronal apoptosis (Herrero-Mendez, Almeida, Fernández, Maestre, Moncada & Bolaños, 2009). The reduction of NADPH levels in the presence of ER-stress might imply the involvement of the ER-stress in downregulation of the PPP and possibly shunting of the glucose away from the PPP. Furthermore, lower levels of NADPH in the presence of ER-stress might also reflect that more NADPH is being used for regeneration, in order to maintain the GSH pool in neurons. Together, these results showed that ATF4 does not affect GSH regeneration.

An alternative explanation as to why WT cells lose GSH more rapidly could be that the WT cells utilize more GSH due to higher oxidative processes. We chose to look at mitochondrial superoxide levels as a measure of ROS in the cells. To confirm that TG treatment affects the mitochondrial bioenergetics, we analyzed different mitochondrial parameters by measuring the oxygen consumption rate (OCR) of neurons using Seahorse Mito Stress test under different treatment conditions. Results showed that certain mitochondrial aspects such as basal respiration and ATP production are affected by TG (Figure 3.5), suggesting that mitochondrial superoxide is an appropriate measure for oxidative processes in this paradigm. After assessing mitochondrial superoxide levels in both WT and ATF4-deficient neurons at baseline and after treatment with TG for 12 and 24 hours, we saw that even though TG treatment seems to be increasing mitochondrial superoxide levels, there are no ATF4-dependent differences under any of the treatment conditions (Figure 3.6). While mitochondrial superoxide seems to be an appropriate measure for ROS production in an ER-stress paradigm, it is possible that other forms of ROS that were not considered are affected by ATF4. Furthermore, it would also be interesting to measure other free radicals that are directly affected by GSH, such as hydroxyl radicals in both WT and ATF4-deficient cultures (Maher, 2005). Taken together, none of these efforts provided an explanation as to why upregulation of ATF4

leads to a more rapid reduction of GSH in WT neurons compared to ATF4-KO cells when GSH synthesis is inhibited in both cultures.

To further investigate this, we measured transcript levels of various GSH related genes including *ChaC1*, *GCL* and *SIC7A11*. ChaC1 protein is important for degrading GSH (Crawford et al, 2015). Analyses of qRT-PCR results showed that ChaC1 is induced in WT cells treated with TG but not ATF4-KO neurons (Figure 3.7a). This finding suggests that WT neurons possibly degrade GSH more rapidly compared to ATF4-KO cells. This might explain why WT cells lose GSH more rapidly compared to ATF4-KO neurons when the *de novo* synthesis of GSH is blocked using BSO (Figure 3.3a). As mentioned earlier, the pattern of GSH loss is reversed in the absence of BSO, suggesting that there is compensatory mechanism through synthesis in the WT cells. We measured 2 different gene transcripts that are important for GSH synthesis: *GCL* and *SIC7A11*. GCL is the enzyme responsible for catalyzing the first step of GSH synthesis: linkage of glutamate and cysteine to produce γ -glutamylcysteine. Our results showed that ER-stress had no effect on *GCL* mRNA levels. SIC7A11 is an important component of system x_c^- , which is a cystine/glutamate antiporter and is important for GSH synthesis since cysteine is the limiting precursor in the process and so the expression of the antiporter is important for maintaining GSH levels (Clemons, Liu, Duong & Phillips, 2017). Recently it has been reported that SIC7A11 is induced in response to glucose starvation, through the activity of ATF4 (Koppula, Zhang, Shi, Li & Gan, 2017). In line with these results, our qRT-PCR data showed that SIC7A11 is induced under ER-stress conditions but only in the WT cells (Figure 3.7c), highlighting the importance of ATF4 for induction of this gene. Therefore, the induction of this gene might be the mechanism by which the WT cells increase the rate of their GSH synthesis and compensate for the GSH loss caused by ChaC1.

4.2 ATF4-dependent cell death under ER-stress conditions is independent of antioxidant depletion

In a previous report by Lange et al (2008), it was shown that the cell death that is seen as a result of ectopic ATF4 overexpression can be ameliorated by treating cells with

an antioxidant such as BHA, suggesting that the ATF4-dependent cell death is due to antioxidant depletion. Therefore, we next examined whether ATF4-dependent cell death observed in an ER-stress paradigm can be alleviated by addition of antioxidants to the culture. Our results showed that addition of antioxidants such as NAC and BHA had no effect on cell viability and it did not protect neurons against ER-stress -induced, cell death (Figure 3.8 a,b). Although the compounds used in these experiments are well-documented antioxidants and to reduce oxidative damage in the cells (Aldini et al, 2018; Lam, Pai & Wattenberg, 1979), it will be important for future experiments to confirm that they effectively reduce oxidative processes in our paradigm.

4.3 ATF4 induces different target genes depending on how it's stabilized/ expressed

The next step was to find an explanation for the differential observations regarding the effects of ectopically overexpressed and endogenously upregulated ATF4 on cellular GSH levels. ATF4 is a bZIP transcription factor, which functions as a heterodimer with other bZIP family transcription factors. It has been shown that different heterodimerization partners can influence the outcome of ATF4 activation (Wang et al, 2009; Ohoka, Yoshii, Hattori, Onozaki & Hayashi, 2005; Huggins et al, 2016). Therefore, ATF4 was stabilized/expressed in 3 different ways in order to assess whether it will have an effect on its transcription of downstream gene targets. The three different ways of expression/stabilization were post-transcriptional modification through the activation of the ISR, post-translational stabilization through inhibition of the proteasome (Milani et al, 2009) and finally ectopic overexpression through plasmid transfection. Analysis of qRT-PCR results showed that indeed the mechanism by which ATF4 is expressed plays a role in differential induction of target genes including GSH related transcripts. For example, our results showed that pro-apoptotic genes such as *CHOP* and *Trib3* are induced when ATF4 is expressed in response to ISR, while *ATF3* is induced more robustly when ATF4 is stabilized post-translationally (Figure 3.10). Similarly, *ChaC1* and *SLC7A11* are also induced more robustly in the presence of ISR-activated ATF4 than post-translationally stabilized or overexpressed form of the protein (Figure

3.11). Furthermore, there are other genes such as *4E-BP1* that is induced in primary cortical neurons but not in N2A cells, suggesting that ATF4 can regulate target genes in a cell-type specific manner (Figure 3.10). Consistent with this, comparison of ATF4 gene expression array data in neurons and fibroblasts has shown that while there is significant overlap in the expression profiles, there is a subset of genes that is regulated in neurons but not in fibroblasts (Lange et al, 2008). This confirms that although ATF4 regulates most of its target genes in a cell type-independent manner, certain genes such as Trib3 are regulated in a cell-type specific manner. This could also partly explain why ATF4 plays a pro-survival role in some cells and a pro-apoptotic role in others. In our results, it is likely that the differences seen in the pattern of target gene induction would be due to interaction of ATF4 with different dimerization partners that differ based on how ATF4 is expressed. Furthermore, considering that ectopic overexpression of ATF4 elevated protein levels of ATF4 substantially, it seems that it is ineffective in terms of target gene induction since none of the transcripts were induced in response to plasmid overexpression. This suggests that stress might be an important aspect for proper heterodimerization, activation and consequently function of ATF4. Unfortunately, in this study we did not have access to viral vector to ectopically express ATF4 in primary neuronal cultures as it would be interesting to determine whether enforced expression of ATF4 in primary neurons is also inefficient in driving target gene transcription. These results may partly explain the differential observations regarding GSH metabolism in neurons.

Additionally, the model used in the study published by Lange and colleagues (2008), employed immature cortical neurons while in our study, we ensured that neurons are matured in culture before conducting any experiments so that our interpretations were more reflective of how mature neurons respond and react to upregulation of ATF4 expression. It is possible that the maturity level of neurons would affect the activity of ATF4 protein or how neurons respond to ATF4 protein induction.

Chapter 5

5 Conclusion

ATF4 has been shown to act as a proapoptotic transcription factor in neurons, however the mechanism by which ATF4 promotes neuronal cell death remains unclear. A previous study suggested that in an overexpression paradigm, ATF4 can promote neuronal cell death by decreasing cellular GSH, leading to oxidative stress-induced apoptosis. In contrast, we found that endogenous upregulation of ATF4 under cell stress conditions promote GSH synthesis and functions to maintain cellular GSH levels. Furthermore, we found that ATF4-dependent cell death induced by ER-stress is not correlated with GSH levels and cannot be ameliorated through replenishment of the cellular antioxidant pool. Taken together, our results suggest that oxidative stress is more likely a causative factor in ATF4 activation as opposed to a consequence. Finally, we suggest that the underlying reason behind the disparity in observations in terms of the effect of ATF4 on GSH levels, may be due to induction of different target genes and possibly different ATF4 heterodimerization partners.

References

- Aime, P., Sun, X., Zareen, N., Rao, A., Berman, Z., & Volpicelli-Daley, L. et al. (2015). Trib3 Is Elevated in Parkinson's Disease and Mediates Death in Parkinson's Disease Models. *Journal Of Neuroscience*, 35(30), 10731-10749. doi: 10.1523/jneurosci.0614-15.2015
- Aldini, G., Altomare, A., Baron, G., Vistoli, G., Carini, M., Borsani, L., & Sergio, F. (2018). N-Acetylcysteine as an antioxidant and disulphide breaking agent: the reasons why. *Free Radical Research*, 52(7), 751-762. doi: 10.1080/10715762.2018.1468564
- Almeida, A., Almeida, J., Bolanos, J., & Moncada, S. (2001). Different responses of astrocytes and neurons to nitric oxide: The role of glycolytically generated ATP in astrocyte protection. *Proceedings Of The National Academy Of Sciences*, 98(26), 15294-15299. doi: 10.1073/pnas.261560998
- Almeida, A., Moncada, S., & Bolaños, J. (2003). Nitric oxide switches on glycolysis through the AMP protein kinase and 6-phosphofructo-2-kinase pathway. *Nature Cell Biology*, 6(1), 45-51. doi: 10.1038/ncb1080
- Amemiya, S., Kamiya, T., Nito, C., Inaba, T., Kato, K., & Ueda, M. et al. (2005). Anti-apoptotic and neuroprotective effects of edaravone following transient focal ischemia in rats. *European Journal Of Pharmacology*, 516(2), 125-130. doi: 10.1016/j.ejphar.2005.04.036
- Ansari, M., & Scheff, S. (2010). Oxidative Stress in the Progression of Alzheimer Disease in the Frontal Cortex. *Journal Of Neuropathology & Experimental Neurology*, 69(2), 155-167. doi: 10.1097/nen.0b013e3181cb5af4
- Badaloo, A., Reid, M., Forrester, T., Heird, W., & Jahoor, F. (2002). Cysteine supplementation improves the erythrocyte glutathione synthesis rate in children with severe edematous malnutrition. *The American Journal Of Clinical Nutrition*, 76(3), 646-652. doi: 10.1093/ajcn/76.3.646

- Bagheri-Yarmand, R., Sinha, K., Gururaj, A., Ahmed, Z., Rizvi, Y., & Huang, S. et al. (2015). A Novel Dual Kinase Function of the RET Proto-oncogene Negatively Regulates Activating Transcription Factor 4-mediated Apoptosis. *Journal Of Biological Chemistry*, 290(18), 11749-11761. doi: 10.1074/jbc.m114.619833
- Baleriola, J., Walker, C., Jean, Y., Crary, J., Troy, C., Nagy, P., & Hengst, U. (2014). Axonally Synthesized ATF4 Transmits a Neurodegenerative Signal across Brain Regions. *Cell*, 158(5), 1159-1172. doi: 10.1016/j.cell.2014.07.001
- Ballatori, N., Krance, S., Notenboom, S., Shi, S., Tieu, K., & Hammond, C. (2009). Glutathione dysregulation and the etiology and progression of human diseases. *Biological Chemistry*, 390(3). doi: 10.1515/bc.2009.033
- Baxter, P., Bell, K., Hasel, P., Kaindl, A., Fricker, M., & Thomson, D. et al. (2015). Synaptic NMDA receptor activity is coupled to the transcriptional control of the glutathione system. *Nature Communications*, 6(1). doi: 10.1038/ncomms7761
- Bélangier, M., Allaman, I., & Magistretti, P. (2011). Brain Energy Metabolism: Focus on Astrocyte-Neuron Metabolic Cooperation. *Cell Metabolism*, 14(6), 724-738. doi: 10.1016/j.cmet.2011.08.016
- Betarbet, R., Sherer, T., MacKenzie, G., Garcia-Osuna, M., Panov, A., & Greenamyre, J. (2000). Chronic systemic pesticide exposure reproduces features of Parkinson's disease. *Nature Neuroscience*, 3(12), 1301-1306. doi: 10.1038/81834
- Bogaerts, V., Theuns, J., & van Broeckhoven, C. (2008). Genetic findings in Parkinson's disease and translation into treatment: a leading role for mitochondria?. *Genes, Brain And Behavior*, 7(2), 129-151. doi: 10.1111/j.1601-183x.2007.00342.x
- Brack, C., Bechter-Thüring, E., & Labuhn, M. (1997). N-Acetylcysteine slows down ageing and increases the life span of *Drosophila melanogaster*. *Cellular And Molecular Life Sciences*, 53(11-12), 960-966. doi: 10.1007/pl00013199
- Bredt, D. (2003). Nitric oxide signaling specificity -- the heart of the problem. *Journal Of Cell Science*, 116(1), 9-15. doi: 10.1242/jcs.00183

Cadenas, E., & Davies, K. (2000). Mitochondrial free radical generation, oxidative stress, and aging. *Free Radical Biology And Medicine*, 29(3-4), 222-230. doi: 10.1016/s08915849(00)00317-8

Cai, Y., Li, J., Yang, S., Li, P., Zhang, X., & Liu, H. (2012). CIBZ, a Novel BTB Domain-Containing Protein, Is Involved in Mouse Spinal Cord Injury via Mitochondrial Pathway Independent of p53 Gene. *Plos ONE*, 7(3), e33156. doi: 10.1371/journal.pone.0033156

Cai, Y., Li, J., Zhang, Z., Chen, J., Zhu, Y., & Li, R. et al. (2017). Zbtb38 is a novel target for spinal cord injury. *Oncotarget*, 8(28). doi: 10.18632/oncotarget.17487

Carlsson, L., Jonsson, J., Edlund, T., & Marklund, S. (1995). Mice lacking extracellular superoxide dismutase are more sensitive to hyperoxia. *Proceedings Of The National Academy Of Sciences*, 92(14), 6264-6268. doi: 10.1073/pnas.92.14.6264

Cassarino, D., & Bennett, J. (1999). An evaluation of the role of mitochondria in neurodegenerative diseases: mitochondrial mutations and oxidative pathology, protective nuclear responses, and cell death in neurodegeneration. *Brain Research Reviews*, 29(1), 1-25. doi: 10.1016/s0165-0173(98)00046-0

Chan, P. (2001). Reactive Oxygen Radicals in Signaling and Damage in the Ischemic Brain. *Journal Of Cerebral Blood Flow & Metabolism*, 21(1), 2-14. doi: 10.1097/00004647-200101000-00002

Chang, R., Wong, A., Ng, H., & Hugon, J. (2002). Phosphorylation of eukaryotic initiation factor-2 α (eIF2 α) is associated with neuronal degeneration in Alzheimer's disease. *Neuroreport*, 13(18), 2429-2432. doi: 10.1097/00001756-200212200-00011

Chen, H., Kim, G., Okami, N., Narasimhan, P., & Chan, P. (2011). NADPH oxidase is involved in post-ischemic brain inflammation. *Neurobiology Of Disease*, 42(3), 341-348. doi: 10.1016/j.nbd.2011.01.027

Chen, H., Song, Y., & Chan, P. (2009). Inhibition of NADPH Oxidase is Neuroprotective after Ischemia—Reperfusion. *Journal Of Cerebral Blood Flow & Metabolism*, 29(7), 1262-1272. doi: 10.1038/jcbfm.2009.47

Chouchani, E., Pell, V., Gaude, E., Aksentijević, D., Sundier, S., & Robb, E. et al. (2014). Ischaemic accumulation of succinate controls reperfusion injury through mitochondrial ROS. *Nature*, 515(7527), 431-435. doi: 10.1038/nature13909

Clark, W., Rinker, L., Lessov, N., Lowery, S., & Cipolla, M. (2001). Efficacy of Antioxidant Therapies in Transient Focal Ischemia in Mice. *Stroke*, 32(4), 1000-1004. doi: 10.1161/01.str.32.4.1000

Clemons, N., Liu, D., Duong, C., & Phillips, W. (2017). Inhibiting system xC⁻ and glutathione biosynthesis – a potential Achilles' heel in mutant-p53 cancers. *Molecular & Cellular Oncology*, 4(5), e1344757. doi: 10.1080/23723556.2017.1344757

Crawford, R., Prescott, E., Sylvester, C., Higdon, A., Shan, J., Kilberg, M., & Mungrue, I. (2015). Human CHAC1 Protein Degrades Glutathione, and mRNA Induction Is Regulated by the Transcription Factors ATF4 and ATF3 and a Bipartite ATF/CRE Regulatory Element. *Journal Of Biological Chemistry*, 290(25), 15878-15891. doi: 10.1074/jbc.m114.635144

Dexter, D., Sian, J., Rose, S., Hindmarsh, J., Mann, V., & Cooper, J. et al. (1994). Indices of oxidative stress and mitochondrial function in individuals with incidental Lewy body disease. *Annals Of Neurology*, 35(1), 38-44. doi: 10.1002/ana.410350107

Drew, R., & Miners, J. (1984). The effects of buthionine sulfoximine (BSO) on glutathione depletion and xenobiotic biotransformation. *Biochemical Pharmacology*, 33(19), 2989-2994. doi: 10.1016/0006-2952(84)90598-7

Dringen, R., & Hamprecht, B. (1999). N-Acetylcysteine, but not methionine or 2-oxothiazolidine-4-carboxylate, serves as cysteine donor for the synthesis of glutathione in cultured neurons derived from embryonal rat brain. *Neuroscience Letters*, 259(2), 79-82. doi: 10.1016/s0304-3940(98)00894-5

- Du, X., Wang, X., & Geng, M. (2018). Alzheimer's disease hypothesis and related therapies. *Translational Neurodegeneration*, 7(1). doi: 10.1186/s40035-018-0107-y
- Ethen, C., Reilly, C., Feng, X., Olsen, T., & Ferrington, D. (2007). Age-Related Macular Degeneration and Retinal Protein Modification by 4-Hydroxy-2-nonenal. *Investigative Ophthalmology & Visual Science*, 48(8), 3469. doi: 10.1167/iovs.06-1058
- Fattman, C., Schaefer, L., & Oury, T. (2003). Extracellular superoxide dismutase in biology and medicine. *Free Radical Biology And Medicine*, 35(3), 236-256. doi: 10.1016/s0891-5849(03)00275-2
- Filomeni, G., Rotilio, G., & Ciriolo, M. (2003). Glutathione disulfide induces apoptosis in U937 cells by a redox-mediated p38 MAP kinase pathway. *The FASEB Journal*, 17(1), 64-66. doi: 10.1096/fj.02-0105fje
- Galano, A., & Alvarez-Idaboy, J. (2011). Glutathione: mechanism and kinetics of its non-enzymatic defense action against free radicals. *RSC Advances*, 1(9), 1763. doi: 10.1039/c1ra00474c
- Galehdar, Z., Swan, P., Fuerth, B., Callaghan, S., Park, D., & Cregan, S. (2010). Neuronal Apoptosis Induced by Endoplasmic Reticulum Stress Is Regulated by ATF4-CHOP-Mediated Induction of the Bcl-2 Homology 3-Only Member PUMA. *Journal Of Neuroscience*, 30(50), 16938-16948. doi: 10.1523/jneurosci.1598-10.2010
- Ghosh, D., LeVault, K., Barnett, A., & Brewer, G. (2012). A Reversible Early Oxidized Redox State That Precedes Macromolecular ROS Damage in Aging Nontransgenic and 3xTg-AD Mouse Neurons. *Journal Of Neuroscience*, 32(17), 5821-5832. doi: 10.1523/jneurosci.6192-11.2012
- Girouard, H., Wang, G., Gallo, E., Anrather, J., Zhou, P., Pickel, V., & Iadecola, C. (2009). NMDA Receptor Activation Increases Free Radical Production through Nitric Oxide and NOX2. *Journal Of Neuroscience*, 29(8), 2545-2552. doi: 10.1523/jneurosci.0133-09.2009

Good, P., Werner, P., Hsu, A., Olanow, W., & Perl., D. (1996). Evidence of neuronal oxidative damage in Alzheimer's disease. *American Journal Of Pathology*. 149 (1), 21-28.

Grant, C., MacIver, F., & Dawes, I. (1997). Glutathione synthetase is dispensable for growth under both normal and oxidative stress conditions in the yeast *Saccharomyces cerevisiae* due to an accumulation of the dipeptide gamma-glutamylcysteine. *Molecular Biology Of The Cell*, 8(9), 1699-1707. doi: 10.1091/mbc.8.9.1699

Gully, J., Sergeyev, V., Bhootada, Y., Mendez-Gomez, H., Meyers, C., & Zolotukhin, S. et al. (2016). Up-regulation of activating transcription factor 4 induces severe loss of dopamine nigral neurons in a rat model of Parkinson's disease. *Neuroscience Letters*, 627, 36-41. doi: 10.1016/j.neulet.2016.05.039

Halliday, M., Radford, H., Sekine, Y., Moreno, J., Verity, N., & le Quesne, J. et al. (2015). Partial restoration of protein synthesis rates by the small molecule ISRIB prevents neurodegeneration without pancreatic toxicity. *Cell Death And Disease*, 6(3), e1672. doi: 10.1038/cddis.2015.49

Halliwell, B. (2001). Role of Free Radicals in the Neurodegenerative Diseases. *Drugs & Aging*, 18(9), 685-716. doi: 10.2165/00002512-200118090-00004

Harding, H., Novoa, I., Zhang, Y., Zeng, H., Wek, R., Schapira, M., & Ron, D. (2000). Regulated Translation Initiation Controls Stress-Induced Gene Expression in Mammalian Cells. *Molecular Cell*, 6(5), 1099-1108. doi: 10.1016/s1097-2765(00)00108-8

Harding, H., Zhang, Y., Bertolotti, A., Zeng, H., & Ron, D. (2000). Perk Is Essential for Translational Regulation and Cell Survival during the Unfolded Protein Response. *Molecular Cell*, 5(5), 897-904. doi: 10.1016/s1097-2765(00)80330-5

Harding, H., Zhang, Y., Zeng, H., Novoa, I., Lu, P., & Calfon, M. et al. (2003). An Integrated Stress Response Regulates Amino Acid Metabolism and Resistance to Oxidative Stress. *Molecular Cell*, 11(3), 619-633. doi: 10.1016/s1097-2765(03)00105-9

- Hauser, D., & Hastings, T. (2013). Mitochondrial dysfunction and oxidative stress in Parkinson's disease and monogenic parkinsonism. *Neurobiology Of Disease*, *51*, 35-42. doi: 10.1016/j.nbd.2012.10.011
- Hayes, J., Flanagan, J., & Jowsey, I. (2005). Glutathione Transferases. *Annual Review Of Pharmacology And Toxicology*, *45*(1), 51-88. doi: 10.1146/annurev.pharmtox.45.120403.095857
- Hensley, K., Hall, N., Subramaniam, R., Cole, P., Harris, M., & Aksenov, M. et al. (2002). Brain Regional Correspondence Between Alzheimer's Disease Histopathology and Biomarkers of Protein Oxidation. *Journal Of Neurochemistry*, *65*(5), 2146-2156. doi: 10.1046/j.1471-4159.1995.65052146.x
- Herrero-Mendez, A., Almeida, A., Fernández, E., Maestre, C., Moncada, S., & Bolaños, J. (2009). The bioenergetic and antioxidant status of neurons is controlled by continuous degradation of a key glycolytic enzyme by APC/C–Cdh1. *Nature Cell Biology*, *11*(6), 747-752. doi: 10.1038/ncb1881
- Hettmann, T., Barton, K., & Leiden, J. (2000). Microphthalmia due to p53-mediated apoptosis of anterior lens epithelial cells in mice lacking the CREB-2 transcription factor. *Developmental Biology*, *222*(1), 110-123. doi: 10.1006/dbio.2000.9699
- Hosoi, T., Kakimoto, M., Tanaka, K., Nomura, J., & Ozawa, K. (2016). Unique pharmacological property of ISRIB in inhibition of A β -induced neuronal cell death. *Journal Of Pharmacological Sciences*, *131*(4), 292-295. doi: 10.1016/j.jphs.2016.08.003
- Huang, Q., Aluise, C., Joshi, G., Sultana, R., St. Clair, D., Markesbery, W., & Butterfield, D. (2010). Potential in vivo amelioration by N-acetyl-L-cysteine of oxidative stress in brain in human double mutant APP/PS-1 knock-in mice: Toward therapeutic modulation of mild cognitive impairment. *Journal Of Neuroscience Research*, n/a-n/a. doi: 10.1002/jnr.22422

- Huggins, C., Mayekar, M., Martin, N., Saylor, K., Gonit, M., & Jailwala, P. et al. (2015). C/EBP γ Is a Critical Regulator of Cellular Stress Response Networks through Heterodimerization with ATF4. *Molecular And Cellular Biology*, 36(5), 693-713. doi: 10.1128/mcb.00911-15
- Hwang, O. (2013). Role of Oxidative Stress in Parkinson's Disease. *Experimental Neurobiology*, 22(1), 11. doi: 10.5607/en.2013.22.1.11
- Jackman, N., Uliasz, T., Hewett, J., & Hewett, S. (2010). Regulation of System xc-Activity and Expression in Astrocytes by Interleukin-1 β . *Glia*, 58(15), 1806-1815. doi: 10.1002/glia.21050
- Jenner, P. (1994). Oxidative damage in neurodegenerative disease. *The Lancet*, 344(8925), 796-798. doi: 10.1016/s0140-6736(94)92347-7
- Karpinski, B., Morle, G., Huggenvik, J., Uhler, M., & Leiden, J. (1992). Molecular cloning of human CREB-2: an ATF/CREB transcription factor that can negatively regulate transcription from the cAMP response element. *Proceedings Of The National Academy Of Sciences*, 89(11), 4820-4824. doi: 10.1073/pnas.89.11.4820
- Karuppagounder, S., Alim, I., Khim, S., Bourassa, M., Sleiman, S., & John, R. et al. (2016). Therapeutic targeting of oxygen-sensing prolyl hydroxylases abrogates ATF4-dependent neuronal death and improves outcomes after brain hemorrhage in several rodent models. *Science Translational Medicine*, 8(328), 328ra29-328ra29. doi: 10.1126/scitranslmed.aac6008
- Khan, M., Sekhon, B., Jatana, M., Giri, S., Gilg, A., & Sekhon, C. et al. (2004). Administration of N-acetylcysteine after focal cerebral ischemia protects brain and reduces inflammation in a rat model of experimental stroke. *Journal Of Neuroscience Research*, 76(4), 519-527. doi: 10.1002/jnr.20087
- Kimball, S. (1999). Eukaryotic initiation factor eIF2. *The International Journal Of Biochemistry & Cell Biology*, 31(1), 25-29. doi: 10.1016/s1357-2725(98)00128-9

- Kondo, T., Reaume, A., Huang, T., Carlson, E., Murakami, K., & Chen, S. et al. (1997). Reduction of CuZn-Superoxide Dismutase Activity Exacerbates Neuronal Cell Injury and Edema Formation after Transient Focal Cerebral Ischemia. *The Journal Of Neuroscience*, 17(11), 4180-4189. doi: 10.1523/jneurosci.17-11-04180.1997
- Koppula, P., Zhang, Y., Shi, J., Li, W., & Gan, B. (2017). The glutamate/cystine antiporter SLC7A11/xCT enhances cancer cell dependency on glucose by exporting glutamate. *Journal Of Biological Chemistry*, 292(34), 14240-14249. doi: 10.1074/jbc.m117.798405
- Krishnamoorthy, T., Pavitt, G., Zhang, F., Dever, T., & Hinnebusch, A. (2001). Tight Binding of the Phosphorylated Subunit of Initiation Factor 2 (eIF2) to the Regulatory Subunits of Guanine Nucleotide Exchange Factor eIF2B Is Required for Inhibition of Translation Initiation. *Molecular And Cellular Biology*, 21(15), 5018-5030. doi: 10.1128/mcb.21.15.5018-5030.2001
- Lam, L., Pai, R., & Wattenberg, L. (1979). Synthesis and chemical carcinogen inhibitory activity of 2-tert-butyl-4-hydroxyanisole. *Journal Of Medicinal Chemistry*, 22(5), 569-571. doi: 10.1021/jm00191a020
- Lange, P., Chavez, J., Pinto, J., Coppola, G., Sun, C., & Townes, T. et al. (2008). ATF4 is an oxidative stress-inducible, prodeath transcription factor in neurons in vitro and in vivo. *The Journal Of Experimental Medicine*, 205(5), 1227-1242. doi: 10.1084/jem.20071460
- Langston, J., Forno, L., Rebert, C., & Irwin, I. (1984). Selective nigral toxicity after systemic administration of 1-methyl-4-phenyl-1,2,5,6-tetrahydropyridine (MPTP) in the squirrel monkey. *Brain Research*, 292(2), 390-394. doi: 10.1016/0006-8993(84)90777-7
- Lassot, I., Estrabaud, E., Emiliani, S., Benkirane, M., Benarous, R., & Margottin-Goguet, F. (2005). p300 Modulates ATF4 Stability and Transcriptional Activity Independently of Its Acetyltransferase Domain. *Journal Of Biological Chemistry*, 280(50), 41537-41545. doi: 10.1074/jbc.m505294200

- Lassot, I., Segéral, E., Berlioz-Torrent, C., Durand, H., Groussin, L., & Hai, T. et al. (2001). ATF4 Degradation Relies on a Phosphorylation-Dependent Interaction with the SCF TrCP Ubiquitin Ligase. *Molecular And Cellular Biology*, 21(6), 2192-2202. doi: 10.1128/mcb.21.6.2192-2202.2001
- Lebovitz, R., Zhang, H., Vogel, H., Cartwright, J., Dionne, L., & Lu, N. et al. (1996). Neurodegeneration, myocardial injury, and perinatal death in mitochondrial superoxide dismutase-deficient mice. *Proceedings Of The National Academy Of Sciences*, 93(18), 9782-9787. doi: 10.1073/pnas.93.18.9782
- Lim, J., & Donaldson, P. (2011). Focus on Molecules: The cystine/glutamate exchanger (System xc⁻). *Experimental Eye Research*, 92(3), 162-163. doi: 10.1016/j.exer.2010.05.007
- Lindenau, J., Noack, H., Asayama, K., & Wolf, G. (1998). Enhanced cellular glutathione peroxidase immunoreactivity in activated astrocytes and in microglia during excitotoxin induced neurodegeneration. *Glia*, 24(2), 252-256. doi: 10.1002/(sici)1098-1136(199810)24:2<252::aid-glia10>3.0.co;2-z
- Liu, C., & Kaufman, R. (2003). The unfolded protein response. *Journal Of Cell Science*, 116(10), 1861-1862. doi: 10.1242/jcs.00408
- Liu, D., & Xu, Y. (2011). p53, Oxidative Stress, and Aging. *Antioxidants & Redox Signaling*, 15(6), 1669-1678. doi: 10.1089/ars.2010.3644
- Lu, P., Jousse, C., Marciniak, S., Zhang, Y., Novoa, I., & Scheuner, D. et al. (2004). Cytoprotection by pre-emptive conditional phosphorylation of translation initiation factor 2. *The EMBO Journal*, 23(1), 169-179. doi: 10.1038/sj.emboj.7600030
- Lu, S. (2013). Glutathione synthesis. *Biochimica Et Biophysica Acta (BBA) - General Subjects*, 1830(5), 3143-3153. doi: 10.1016/j.bbagen.2012.09.008
- Luo, S., Baumeister, P., Yang, S., Abcouwer, S., & Lee, A. (2003). Induction of Grp78/BiP by Translational Block. *Journal Of Biological Chemistry*, 278(39), 37375-37385. doi: 10.1074/jbc.m303619200

- Ma, T., Trinh, M., Wexler, A., Bourbon, C., Gatti, E., & Pierre, P. et al. (2013). Suppression of eIF2 α kinases alleviates Alzheimer's disease-related plasticity and memory deficits. *Nature Neuroscience*, 16(9), 1299-1305. doi: 10.1038/nn.3486
- Ma, Y., & Hendershot, L. (2003). Delineation of a Negative Feedback Regulatory Loop That Controls Protein Translation during Endoplasmic Reticulum Stress. *Journal Of Biological Chemistry*, 278(37), 34864-34873. doi: 10.1074/jbc.m301107200
- Machado, A., Ayala, A., Gordillo, E., Revilla, E., & Santa Maria, C. (1991). Relationship between enzymatic activity loss and post-translational protein modification in aging. *Archives Of Gerontology And Geriatrics*, 12(2-3), 187-197. doi: 10.1016/0167-4943(91)90027-n
- Maher, P. (2005). The effects of stress and aging on glutathione metabolism. *Ageing Research Reviews*, 4(2), 288-314. doi: 10.1016/j.arr.2005.02.005
- Mandal, P., Tripathi, M., & Sugunan, S. (2012). Brain oxidative stress: Detection and mapping of anti-oxidant marker 'Glutathione' in different brain regions of healthy male/female, MCI and Alzheimer patients using non-invasive magnetic resonance spectroscopy. *Biochemical And Biophysical Research Communications*, 417(1), 43-48. doi: 10.1016/j.bbrc.2011.11.047
- Mari, M., Morales, A., Colell, A., García-Ruiz, C., & Fernández-Checa, J. (2009). Mitochondrial Glutathione, a Key Survival Antioxidant. *Antioxidants & Redox Signaling*, 11(11), 2685-2700. doi: 10.1089/ars.2009.2695
- Marcus, D., Thomas, C., Rodriguez, C., Simberkoff, K., Tsai, J., Strafaci, J., & Freedman, M. (1998). Increased Peroxidation and Reduced Antioxidant Enzyme Activity in Alzheimer's Disease. *Experimental Neurology*, 150(1), 40-44. doi: 10.1006/exnr.1997.6750
- Masuoka, H., & Townes, T. (2002). Targeted disruption of the activating transcription factor 4 gene results in severe fetal anemia in mice. *Blood*, 99(3), 736-745. doi: 10.1182/blood.v99.3.736

- McCann, S., Dusting, G., & Roulston, C. (2008). Early increase of Nox4 NADPH oxidase and superoxide generation following endothelin-1-induced stroke in conscious rats. *Journal Of Neuroscience Research*, 86(11), 2524-2534. doi: 10.1002/jnr.21700
- Miaji, Y., Yoshimura, S., Sakai, N., Yamagami, H., Egashira, Y., & Shirakawa, M. et al. (2015). Effect of Edoxone on Favorable Outcome in Patients with Acute Cerebral Large Vessel Occlusion: Subanalysis of RESCUE-Japan Registry. *Neurologia Medico-Chirurgica*, 55(3), 241-247. doi: 10.2176/nmc.ra.2014-0219
- Mikawa, S., Kinouchi, H., Kamii, H., Gobbel, G., Chen, S., & Carlson, E. et al. (1996). Attenuation of acute and chronic damage following traumatic brain injury in copper, zinc—superoxide dismutase transgenic mice. *Journal Of Neurosurgery*, 85(5), 885-891. doi: 10.3171/jns.1996.85.5.0885
- Milani, M., Rzymiski, T., Mellor, H., Pike, L., Bottini, A., Generali, D., & Harris, A. (2009). The Role of ATF4 Stabilization and Autophagy in Resistance of Breast Cancer Cells Treated with Bortezomib. *Cancer Research*, 69(10), 4415-4423. doi: 10.1158/0008-5472.can-08-2839
- Ohoka, N., Yoshii, S., Hattori, T., Onozaki, K., & Hayashi, H. (2005). TRB3, a novel ER stress-inducible gene, is induced via ATF4—CHOP pathway and is involved in cell death. *The EMBO Journal*, 24(6), 1243-1255. doi: 10.1038/sj.emboj.7600596
- Pacelli, C., Giguère, N., Bourque, M., Lévesque, M., Slack, R., & Trudeau, L. (2015). Elevated Mitochondrial Bioenergetics and Axonal Arborization Size Are Key Contributors to the Vulnerability of Dopamine Neurons. *Current Biology*, 25(18), 2349-2360. doi: 10.1016/j.cub.2015.07.050
- Pakos-Zebrucka, K., Koryga, I., Mnich, K., Ljubic, M., Samali, A., & Gorman, A. (2016). The integrated stress response. *EMBO Reports*, 17(10), 1374-1395. doi: 10.15252/embr.201642195

- Palmer, A., & Burns, M. (1994). Selective increase in lipid peroxidation in the inferior temporal cortex in Alzheimer's disease. *Brain Research*, 645(1-2), 338-342. doi: 10.1016/0006-8993(94)91670-5
- Perier, C., & Vila, M. (2011). Mitochondrial Biology and Parkinson's Disease. *Cold Spring Harbor Perspectives In Medicine*, 2(2), a009332-a009332. doi: 10.1101/cshperspect.a009332
- Podust, L., Krezel, A., & Kim, Y. (2000). Crystal Structure of the CCAAT Box/Enhancer-binding Protein β Activating Transcription Factor-4 Basic Leucine Zipper Heterodimer in the Absence of DNA. *Journal Of Biological Chemistry*, 276(1), 505-513. doi: 10.1074/jbc.m005594200
- Prasad, M., Lovell, M., Yatin, M., Dhillon, H., & Markesbery, W. (1998). *Neurochemical Research*, 23(1), 81-88. doi: 10.1023/a:1022457605436
- Reid, M., Badaloo, A., Forrester, T., Morlese, J., Frazer, M., Heird, W., & Jahoor, F. (2000). In vivo rates of erythrocyte glutathione synthesis in children with severe protein-energy malnutrition. *American Journal Of Physiology-Endocrinology And Metabolism*, 278(3), E405-E412. doi:10.1152/ajpendo.2000.278.3.e405
- Resende, R., Moreira, P., Proença, T., Deshpande, A., Busciglio, J., Pereira, C., & Oliveira, C. (2008). Brain oxidative stress in a triple-transgenic mouse model of Alzheimer disease. *Free Radical Biology And Medicine*, 44(12), 2051-2057. doi: 10.1016/j.freeradbiomed.2008.03.012
- Rogers, T., Inesi, G., Wade, R., & Lederer, W. (1995). Use of thapsigargin to study Ca^{2+} homeostasis in cardiac cells. *Bioscience Reports*, 15(5), 341-349. doi: 10.1007/bf01788366
- Ryu, E., Angelastro, J., & Greene, L. (2005). Analysis of gene expression changes in a cellular model of Parkinson disease. *Neurobiology Of Disease*, 18(1), 54-74. doi: 10.1016/j.nbd.2004.08.016

- Ryu, E., Harding, H., Angelastro, J., Vitolo, O., Ron, D., & Greene, L. (2002). Endoplasmic Reticulum Stress and the Unfolded Protein Response in Cellular Models of Parkinson's Disease. *The Journal Of Neuroscience*, 22(24), 10690-10698. doi: 10.1523/jneurosci.22-24-10690.2002
- Sagara, J., Miura, K., & Bannai, S. (1993). Maintenance of Neuronal Glutathione by Glial Cells. *Journal Of Neurochemistry*, 61(5), 1672-1676. doi: 10.1111/j.1471-4159.1993.tb09802.x
- Saleem, S., & Biswas, S. (2016). Tribbles Pseudokinase 3 Induces Both Apoptosis and Autophagy in Amyloid- β -induced Neuronal Death. *Journal Of Biological Chemistry*, 292(7), 2571-2585. doi: 10.1074/jbc.m116.744730
- Scortegagna, M., Kim, H., Li, J., Yao, H., Brill, L., & Han, J. et al. (2014). Fine Tuning of the UPR by the Ubiquitin Ligases Siah1/2. *Plos Genetics*, 10(5), e1004348. doi: 10.1371/journal.pgen.1004348
- Sekhar, R., Patel, S., Guthikonda, A., Reid, M., Balasubramanyam, A., Taffet, G., & Jahoor, F. (2011). Deficient synthesis of glutathione underlies oxidative stress in aging and can be corrected by dietary cysteine and glycine supplementation. *American Journal Of Clinical Nutrition*, 94(3), 847-853. doi: 10.3945/ajcn.110.003483
- Sheng, H., Brady, T., Pearlstein, R., Crapo, J., & Warner, D. (1999). Extracellular superoxide dismutase deficiency worsens outcome from focal cerebral ischemia in the mouse. *Neuroscience Letters*, 267(1), 13-16. doi: 10.1016/s0304-3940(99)00316-x
- Shirley, R., Ord, E., & Work, L. (2014). Oxidative Stress and the Use of Antioxidants in Stroke. *Antioxidants*, 3(3), 472-501. doi: 10.3390/antiox3030472
- Sian, J., Dexter, D., Lees, A., Daniel, S., Agid, Y., & Javoy-Agid, F. et al. (1994). Alterations in glutathione levels in Parkinson's disease and other neurodegenerative disorders affecting basal ganglia. *Annals Of Neurology*, 36(3), 348-355. doi: 10.1002/ana.410360305

Sidrauski, C., Tsai, J., Kampmann, M., Hearn, B., Vedantham, P., & Jaishankar, P. et al. (2015). Pharmacological dimerization and activation of the exchange factor eIF2B antagonizes the integrated stress response. *Elife*, 4. doi: 10.7554/elife.07314

Smith, M., Richey Harris, P., Sayre, L., Beckman, J., & Perry, G. (1997). Widespread Peroxynitrite-Mediated Damage in Alzheimer's Disease. *The Journal Of Neuroscience*, 17(8), 2653-2657. doi: 10.1523/jneurosci.17-08-02653.1997

Sonenberg, N., & Hinnebusch, A. (2009). Regulation of Translation Initiation in Eukaryotes: Mechanisms and Biological Targets. *Cell*, 136(4), 731-745. doi: 10.1016/j.cell.2009.01.042

Swerdlow, R., Burns, J., & Khan, S. (2014). The Alzheimer's disease mitochondrial cascade hypothesis: Progress and perspectives. *Biochimica Et Biophysica Acta (BBA) - Molecular Basis Of Disease*, 1842(8), 1219-1231. doi: 10.1016/j.bbadis.2013.09.010

Tanaka, T., Tsujimura, T., Takeda, K., Sugihara, A., Maekawa, A., & Terada, N. et al. (1998). Targeted disruption of ATF4 discloses its essential role in the formation of eye lens fibres. *Genes To Cells*, 3(12), 801-810. doi: 10.1046/j.1365-2443.1998.00230.x

Teufel, D., Freund, S., Bycroft, M., & Fersht, A. (2007). Four domains of p300 each bind tightly to a sequence spanning both transactivation subdomains of p53. *Proceedings Of The National Academy Of Sciences*, 104(17), 7009-7014. doi: 10.1073/pnas.0702010104

Tönnies, E., & Trushina, E. (2017). Oxidative Stress, Synaptic Dysfunction, and Alzheimer's Disease. *Journal Of Alzheimer's Disease*, 57(4), 1105-1121. doi: 10.3233/jad-161088

Tsuru-Aoyagi, K., Potts, M., Trivedi, A., Pfankuch, T., Raber, J., & Wendland, M. et al. (2009). Glutathione peroxidase activity modulates recovery in the injured immature brain. *Annals Of Neurology*, 65(5), 540-549. doi: 10.1002/ana.21600

Uttara, B., Singh, A., Zamboni, P., & Mahajan, R. (2009). Oxidative Stress and Neurodegenerative Diseases: A Review of Upstream and Downstream Antioxidant

Therapeutic Options. *Current Neuropharmacology*, 7(1), 65-74. doi: 10.2174/157015909787602823

Valentine, J., Doucette, P., & Zittin Potter, S. (2005). Copper-zinc superoxide dismutase and amyotrophic lateral sclerosis. *Annual Review Of Biochemistry*, 74(1), 563-593. doi: 10.1146/annurev.biochem.72.121801.161647

Vallejo, M., Ron, D., Miller, C., & Habener, J. (1993). C/ATF, a member of the activating transcription factor family of DNA-binding proteins, dimerizes with CAAT/enhancer-binding proteins and directs their binding to cAMP response elements. *Proceedings Of The National Academy Of Sciences*, 90(10), 4679-4683. doi: 10.1073/pnas.90.10.4679

Vattem, K., & Wek, R. (2004). Reinitiation involving upstream ORFs regulates ATF4 mRNA translation in mammalian cells. *Proceedings Of The National Academy Of Sciences*, 101(31), 11269-11274. doi: 10.1073/pnas.0400541101

Wang, Q., Mora-Jensen, H., Weniger, M., Perez-Galan, P., Wolford, C., & Hai, T. et al. (2009). ERAD inhibitors integrate ER stress with an epigenetic mechanism to activate BH3-only protein NOXA in cancer cells. *Proceedings Of The National Academy Of Sciences*, 106(7), 2200-2205. doi: 10.1073/pnas.0807611106

Wortel, I., van der Meer, L., Kilberg, M., & van Leeuwen, F. (2017). Surviving Stress: Modulation of ATF4-Mediated Stress Responses in Normal and Malignant Cells. *Trends In Endocrinology & Metabolism*, 28(11), 794-806. doi: 10.1016/j.tem.2017.07.003

Wu, G., Fang, Y., Yang, S., Lupton, J., & Turner, N. (2004). Glutathione Metabolism and Its Implications for Health. *The Journal Of Nutrition*, 134(3), 489-492. doi: 10.1093/jn/134.3.489

Yang, X., Matsuda, K., Bialek, P., Jacquot, S., Masuoka, H., & Schinke, T. et al. (2004). ATF4 Is a Substrate of RSK2 and an Essential Regulator of Osteoblast Biology. *Cell*, 117(3), 387-398. doi: 10.1016/s0092-8674(04)00344-7

Yant, L., Ran, Q., Rao, L., Van Remmen, H., Shibatani, T., & Belter, J. et al. (2003). The selenoprotein GPX4 is essential for mouse development and protects from radiation and oxidative damage insults. *Free Radical Biology And Medicine*, 34(4), 496-502. doi: 10.1016/s0891-5849(02)01360-6

Yuniati, L., van der Meer, L., Tijchon, E., Schenau, D., van Emst, L., & Levers, M. et al. (2016). Tumor suppressor BTG1 promotes PRMT1-mediated ATF4 function in response to cellular stress. *Oncotarget*, 7(3). doi: 10.18632/oncotarget.6519

Zinszner, H., Kuroda, M., Wang, X., Batchvarova, N., Lightfoot, R., & Remotti, H. et al. (1998). CHOP is implicated in programmed cell death in response to impaired function of the endoplasmic reticulum. *Genes & Development*, 12(7), 982-995. doi: 10.1101/gad.12.7.982

Appendices

Appendix A. NADPH reaction mix

Reagent	Standards and Samples
NADPH Cycling Buffer	97 μ L
NADPH Cycling Enzyme Mix	2 μ L
High-sensitivity Probe	1 μ L

Appendix B. qRT-PCR primer list

	Forward Sequence	Reverse Sequence
4eBP1	GGGGACTACAGCACCACTC	GTTCCGACACTCCATCAGAAAT
ATF3	CCCCTGGAGATGTCAGTCAC	GCAGGCACTCTGTCTTCTCC
ChaC1	ACAAGATGCCTGGCCGAGTG	AGGTACTTCAGGGCCTCGTT
CHOP	ACAGAGGTCACACGCACATC	GGGCAGTGACCACTCTGTTT
GADD45	CTGCTGCTACTGGAGAACGAC	CGACTTTCCCGGCAAAAACAAA
GCL	TGGGCACAGGTAAAACCCAA	CTGGGCTTCAATGTCAGGGA
GR	TGGCACTTGCGTGAATGTTG	CGAATGTTGCATAGCCGTGG
S12	GGAAGGCATAGCTGCTGG	CCTCGATGACATCCTTGG
SIC7A11	TTTGGAGCCCTGTCCTATGC	GCTCCAGGGCGTATTACGAG
Trib3	TGCAGGAAGAAACCGTTGGAG	CTCGTTTTAGGACTGGACACTT

Curriculum Vitae

Name: Fatemeh Mirshafiei Langari

Post-secondary Education and Degrees: American University of Sharjah
Sharjah, United Arab Emirates
2011-2015 B.Sc.

The University of Western Ontario
London, Ontario, Canada
2016-2018 M.Sc.

Related Work Experience Physiology Teaching Assistant
The University of Western Ontario
2017 PHYS 4730B
2017-2018 PHYS 3140A
2018 PHYS 4730B

Publications:

Dalibalta, S., **Mirshafiei, F.**, & Davison, G. (2017). Exercise intervention on cardiovascular disease risk factors in a university population in the United Arab Emirates. International Journal of Adolescent Medicine and Health. doi: 10.1515/ijamh-2016-0132